

Fall 9-2012

The Role of MK-STYX in Stress Granule Assembly/Disassembly

Justin Barr

College of William and Mary

Follow this and additional works at: <https://scholarworks.wm.edu/honorsthesis>

Recommended Citation

Barr, Justin, "The Role of MK-STYX in Stress Granule Assembly/Disassembly" (2012). *Undergraduate Honors Theses*. Paper 863.

<https://scholarworks.wm.edu/honorsthesis/863>

This Honors Thesis is brought to you for free and open access by the Theses, Dissertations, & Master Projects at W&M ScholarWorks. It has been accepted for inclusion in Undergraduate Honors Theses by an authorized administrator of W&M ScholarWorks. For more information, please contact scholarworks@wm.edu.

The Role of MK-STYX in Stress Granule Assembly/Disassembly


A thesis submitted in partial fulfillment of the requirement for the degree of
Bachelor of Science in the Department of Biology from
The College of William and Mary

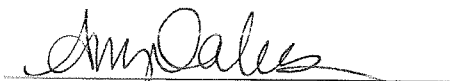
Jamie Barr

Accepted for Honors


Dr. Shantá Hinton, Advisor


Dr. Lizabeth Allison


Dr. Mark Forsyth


Dr. Amy Oakes

Williamsburg, Virginia
April 24, 2012

ABSTRACT

Regulation of cell signaling is critical for determining fundamental processes such as whether a cell will grow, change shape, differentiate or die. Phosphorylation is a post-translational modification of proteins that is key for transducing signaling messages. The major players in phosphorylation cascades are proteins called kinases and phosphatases. Pseudokinases and pseudophosphatases are catalytically inactive proteins that add complexity to the regulation of cell signaling. In this thesis, the pseudophosphatase MK-STYX [MAPK (mitogen-activated protein kinase) phosphoserine/threonine/tyrosine-binding protein] is implicated in the stress response pathway. MK-STYX interacts with G3BP-1 (Ras-GTPase activating protein SH3 domain binding protein-1), and inhibits stress granule assembly. Stress granules, cytoplasmic storage sites for mRNA, form as a protective mechanism against stressors such as UV irradiation, hypoxia, and heat shock. In addition, the overexpression of G3BP-1 induces stress granule assembly. The initial hypothesis for how MK-STYX attenuates stress granule assembly was through a mechanism dependent on the phosphorylation status of G3BP-1 at serine 149. However, data with a G3BP-1 phosphomimetic mutant suggests differently. The eukaryotic initiation factor 2 alpha ($eIF2\alpha$) is investigated for playing a role in the reduction of stress granules by MK-STYX. $eIF2\alpha$ initiates translation by forming a ternary complex with methionine bound to tRNA. Phosphorylation of $eIF2\alpha$ arrests translation and results in stress granule formation, whereas dephosphorylation promotes

polysomes. To determine if MK-STYX inhibits stress granule assembly via upstream interactions, we investigated its effects on eIF2 α phosphorylation. HeLa cells were transfected with pMT2-FLAG-MK-STYX-FLAG or pMT2 expression vectors, and heat shocked for an hour to induce stress. Cells were lysed and immunoblots for phosphorylation of eIF2 α were performed. We show that the presence of MK-STYX reduced the phosphorylation of eIF2 α . Also, MK-STYX was immunoprecipitated with eIF2 α , suggesting that MK-STYX and eIF2 α interact. These data are significant because they suggest MK-STYX may play a role in stress granule assembly. MK-STYX involvement in disassembly was also investigated by immunoblotting for Hsp70. Hsp70 is thought to be necessary for stress granule disassembly and reduces protein aggregation. The overexpression of MK-STYX correlates with increased expression of Hsp70, suggesting MK-STYX may also play a role in stress granule disassembly. This thesis implicates MK-STYX, a pseudophosphatase, as a regulator of cellular processes.

ACKNOWLEDGMENTS

This research and thesis have been a great learning experience and I would like to thank the William and Mary Biology Department for making research opportunities accessible for undergraduates. The mentorship of Professor Shantá D. Hinton has been invaluable, and I cannot thank her enough for helping me realize the goals that I can achieve. The guidance received from Professor Liz Allison and Professor Mark Forsyth has shaped my academic endeavors throughout college and I am grateful for that. Also, thanks to Vinny Roggero for his assistance in the lab. I would like to thank the Hinton Lab and the Allison Lab for the fun times and companionship on numerous coffee runs. Lastly, I thank my friends and family for always supporting my goals.

Table of Contents

Introduction	1
Phosphorylation and cell signaling	1
Protein tyrosine phosphatases.....	2
MAP Kinase Phosphatases.....	6
Pseudophosphatases	8
MK-STYX	10
G3BP.....	12
Stress granule formation	13
Eukaryotic initiation factor 2 alpha	19
Stress granule life cycle	21
Heat Shock Response.....	22
MK-STYX and stress granules	23
Thesis objectives	24
Methods	26
Plasmids.....	26
Cell culture, transfection and heat shock	26
Cell Imaging.....	26
Immunoblotting	27
Immunoprecipitation.....	27
BLAST	28
I-TASSER and StarBiochem	28
Microarray	29
Subcloning: MK-STYX-Cherry	30
Results	32
MK-STYX attenuates stress granule formation independently of G3BP-1 phosphorylation status.....	32
MK-STYX decreases eIF2 α phosphorylation and interacts with eIF2 α	35
MK-STYX increases Hsp70 expression	36
Sequence comparison: BLAST	37
Strucutral comparison: I-TASSER	40
Microarray.....	43
Discussion	47
References	56

INTRODUCTION

“Signal transduction pathways dictate whether a cell will grow and divide, change shape, move, differentiate, or die. The regulation of phosphorylation is critical for homeostasis” (Neel and Tonks, 1997).

Phosphorylation and Cell Signaling

Cell signaling is a form of communication in which molecules transmit information to regulate cell function. Cell signaling is often communicated by phosphorylation of proteins, and this communication is key to maintaining integrity of cell function. Proteins are polymers of amino acids and the “workers” of the cell. Proteins are necessary for maintaining metabolic pathways, signal transduction and structural support. Phosphorylation—the addition of a phosphate group to an amino acid residue, most commonly serine, threonine or tyrosine—is the most common form of post-translational modification of proteins. Phosphorylation is an important mechanism of cell signaling because it can change the conformation of a protein, cause activation or deactivation of a protein, and expose new binding sites for complexes to form. Phosphorylation cascades are controlled by kinases and phosphatases, which work in opposition to regulate cell signaling. Kinases are enzymes that regulate phosphorylation by adding a phosphate group, and phosphatases are enzymes that remove a phosphate group. Kinases control the amplitude of the signaling response, while

phosphatases regulate the rate and duration of the response (Heinrich et al., 2002). Protein phosphatases have evolved multiple times from separate families, unlike protein kinases, which are all derived from a common ancestor (Tonks, 2006). Pseudokinases and pseudophosphatases are structurally related to active homologs, however, they lack critical residues necessary for enzymatic activity.

Protein Tyrosine Phosphatases

Protein tyrosine phosphatases (PTPs) are a superfamily of enzymes that work in opposition of protein tyrosine kinases (PTKs) to regulate phosphorylation events. The PTP superfamily is the largest family of phosphatase genes, and these enzymes are characterized by the active site signature motif HCX₅R (letter code for amino acids, where X represents any amino acid). The cysteine residue is key for nucleophilic attack and removal of the phosphate group (Denu et al., 1996). Removal of the phosphate group is a two-step process. The first step is a nucleophilic attack on the phosphate by the sulfur atom of the thiolate ion of the cysteine residue. This forms a cysteinyl-phosphate intermediate, which is stabilized by a neighboring arginine residue. The arginine residue protonates the P-O bond of the substrate that attaches the phosphate group to an amino acid residue. The second step is the hydrolysis of the phospho-enzyme intermediate, which is mediated by water. Oxidation of the catalytic cysteine inhibits its function

as a nucleophile, and PTP regulation by oxidation in addition to phosphorylation states is a current area of research for the study of phosphatases.

There are approximately 100 human PTP genes in the superfamily, and many of these genes are alternatively spliced, resulting in a complex network of phosphatase regulation of cell signaling pathways (Tonks, 2006). PTPs illustrate both positive and negative regulation of signal transduction. The PTP superfamily is divided into classes: classical PTPs, which are pTyr-specific, and dual specificity phosphatases (DSPs), which are pTyr-specific as well as pSer/Thr-specific. Classical PTPs can be transmembrane receptor-like PTPs or non-transmembrane PTP subfamilies (Neel and Tonks, 1997). There are approximately 65 human genes encoding DSPs, and DSPs have greater structural diversity than the classical PTPs (Tonks, 2006). DSPs are less conserved and have little sequence similarity beyond the signature motif. The DSP active site is shallow, which allows binding to pSer, pThr and pTyr residues. The MKPs (MAP [mitogen activated protein] Kinase Phosphatases) are a subdivision of DSPs. MKPs are well characterized and dephosphorylate MAPKs (MAP Kinases). DSPs have diverse cellular functions; the myotubularins (MTMs) and phosphatase and tensin homologs (PTENs) dephosphorylate non-protein substrates, such as lipids (Begley and Dixon, 2005). The Slingshot subfamily of DSPs are involved in actin de-polymerization, and Cdc14s are implicated in cell cycle progression.

In the era of genomics, high-throughput technology allowed researchers to identify genes of the PTP superfamily. However, the function of many of these genes remains to be elucidated (Andersen et al., 2004). Substrate trapping mutants have been used by researchers to reliably determine substrates that are dephosphorylated by PTPs. Mutating the critical cysteine of the signature motif to a serine allows the PTP to bind pTyr residues; however, catalysis cannot occur. Substrate trapping mutants bind to substrates in the cell, but because they are unable to dephosphorylate targets, the mutant is locked in a stable complex. That allows researchers to identify *bona fide* substrate. (Blanchetot et al., 2005). This technique has been refined by an additional mutation of a conserved aspartate to alanine, which is advantageous in creating a substrate trap and also allowing the formation of the cysteine-phosphate intermediate (Flint et al., 1997).

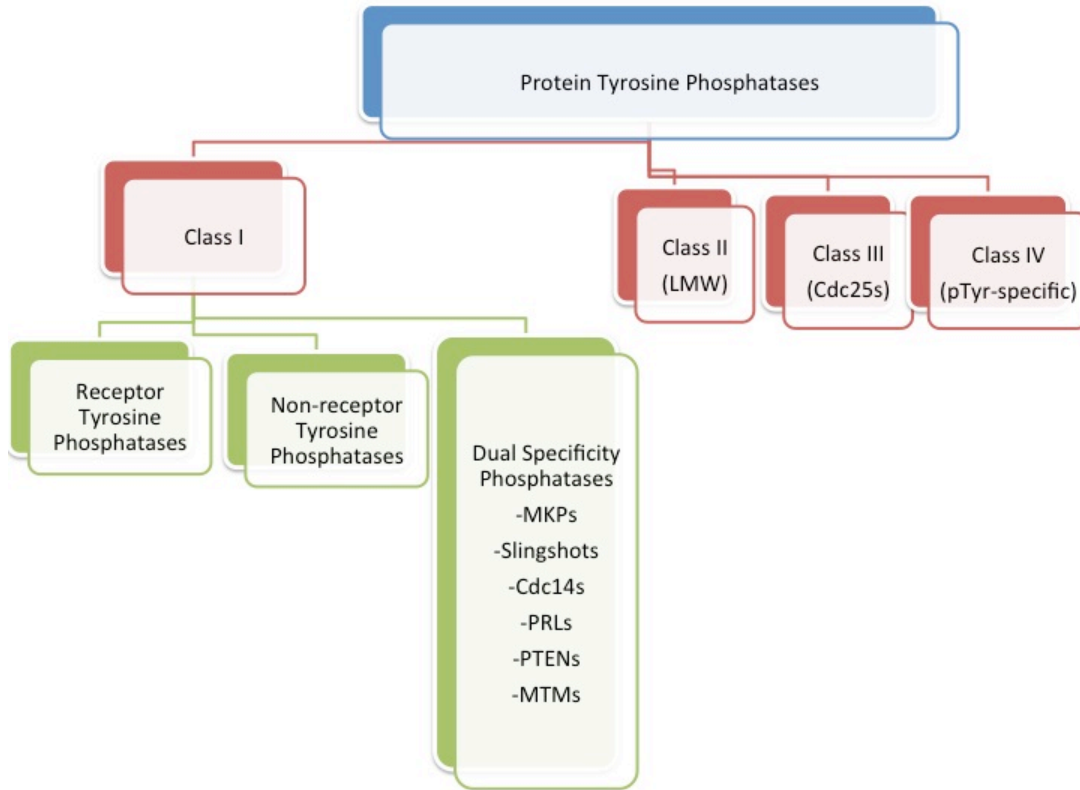


Figure 1. Protein Tyrosine Phosphatases. There are four classes of PTPs. The first class includes classical PTPs: receptor tyrosine phosphatases and nonreceptor tyrosine phosphatases, as well as dual specificity phosphatases (DSPs). DSPs include MAP Kinase Phosphatases (MKPs), Slingshots, Cdc14s, PRLs (phosphatase of regenerating liver 1-3), PTENs (phosphatase and tensin homologs), and MTMs (myotubularins). Class II PTPs are low molecular weight (LMW) phosphatases. Class III includes Cdc25A, B, and C, which are involved in cell cycle regulation. Class IV includes four phosphatases that specifically dephosphorylate tyrosine residues, Eya1, 2, 3, and 4.

MAP Kinase Phosphatases (MKPs)

MKPs are a family of ten dual specificity phosphatases of the PTP superfamily that dephosphorylate MAP kinases. MAP kinase activation requires phosphorylation on threonine and tyrosine residues located within the activation loop of kinase subdomain VIII (Camps et al., 2000). Phosphorylation is a reversible post-translational modification, even in the continued presence of activating stimuli. MKPs show specificity for their substrate by localizing to different subcellular compartments and by differentiating between MAPK isoforms (Camps et al., 2000). The N-terminal domains of MKPs, which are non-catalytic, have two short regions of sequence similarity and are called the CH2 (Cdc25 homology 2) regions. The function of the CH2 domains is not fully understood, but it is implied that they are responsible for the specificity of the MKP-MAPK interactions (Muda et al., 1998). Apart from substrate recognition, it is also suggested that the N-terminal CH2 region can enhance the enzymatic activity of the catalytic PTP domain by causing a conformational change within the C-terminal catalytic domain (Camps et al., 1998; Owens and Keyse, 2007).

MKPs can recognize a specific class of MAPK; for example, MKP3 specifically dephosphorylates the extracellular signal regulated kinase (ERK). MKPs can also regulate multiple MAPK pathways. MKP-1 dephosphorylates both ERK and p38. Transcriptional regulation of MKPs is highly regulated, which leads

to complex regulatory networks in which MAPK signaling is subjected to negative feedback control (Owens and Keyse, 2007).

MAPK signaling pathways respond to many extracellular signals and result in diverse responses, such as cell proliferation, differentiation, stress response, inflammation, growth arrest and apoptosis. There are three major MAPK pathways. The first is the ERK 1 and 2 pathway, which is activated in response to growth factors and hormones. The second and third pathways respond to stress: the c-Jun amino-terminal kinases (JNKs 1-3) and the p38 MAPKs. The core MAPK signaling cascade is composed of three-tiers: MAPK kinase kinase (MKKK or MEKK), phosphorylates MAPK kinase (MKK or MEK), which activates MAPK by phosphorylating both the threonine and tyrosine residues of the conserved T-X-Y motif (Owens and Keyse, 2007).

MKPs are well characterized as regulators of MAPK signaling, and the importance of MKPs as regulators of cell homeostasis is under research. An experiment in 1996 knocked out the MKP-1 gene, and there was no detectable phenotype in the knockout animals or cells (Dorfmann et al., 1996). This led researchers to conclude that MKP-1 is unimportant in cell signaling. However, further knockouts demonstrate that MKP-1 plays a non-redundant role in immune function, and further study of MKPs has deemed them essential for developmental processes (Owens and Keyse, 2007).

Pseudophosphatases

The PTP family also consists of pseudophosphatases. Pseudophosphatases have the conserved core domain of the PTP family, but lack critical residues for enzymatic activity. The conservation of the PTP fold has been demonstrated by mutating the pseudophosphatase residues to generate a catalytically active phosphatase. PTPs appear to be an example of gene duplication and variation giving rise to both catalytic and non-catalytic functional domains (Wishart and Dixon, 1998).

The well-studied pseudophosphatase prototype is Styx, which lacks the critical cysteine and instead has a glycine. Styx plays a functional role; mice with germline mutations in Styx are defective for sperm production (Wishart and Dixon, 2002). Because of the prototype Styx, “STYX” has been coined as the name for a protein domain that is catalytically inactive and resembles PTP domains (Wishart and Dixon, 1998). STYX is named purposefully after the river for the dead in Greek mythology. STYX domains serve to bind phosphorylated residues, just as Src-homology 2 (SH2) and phosphotyrosine interaction/binding (PTB) domains bind phosphorylated residues and mediate protein associations (Wishart and Dixon, 1998). Proteins with STYX domains should not be overlooked as nonfunctional homologs, but rather should be viewed as proteins with conserved modules that are likely to be involved in non-phosphatase functions and mediate protein interactions (Wishart and Dixon, 1998).

Pseudophosphatases are often described as having “dominant-negative” function, by blocking access of the catalytically active phosphatase and protecting substrates from dephosphorylation. Tonks (2009) points out that use of the term “dominant-negative” may create a false impression. A primary function of phosphorylation events is to create docking sites for signaling molecules to bind. This leads to the assembly of multiprotein complexes. Dephosphorylation by active phosphatases could prevent these functional complexes from forming. The advantages of pseudophosphatase signaling regulation are unknown, but are hypothesized as creating multi-protein complexes. Researchers in this field hope to elucidate the subtleties that add to the complexity of cell signaling.

The ability of a PTP to target substrate is not dependent on the catalytic cysteine, which forms the basis for the “substrate trapping” mutant techniques. An interesting effect of the MKP-1 catalytically impaired mutant (cysteine mutated to serine) is that this mutant inhibits cell signaling by sequestering all MKP-1 substrate (Sun et al., 1993). This suggests the possibility that endogenous catalytically inactive phosphatases can function as modulators of cell signaling. Pseudophosphatases are not the only ‘inactive’ members of the phosphorylation cascade; pseudokinases exist as well. In fact, approximately 10 percent of all kinase genes encode pseudokinases (Boudeau et al., 2006), showing the potential that catalytically inactive proteins play a dual-faceted role in regulation of phosphorylation events.

Pseudophosphatases are most common among the myotubularins (MTMs); 6 of 14 phosphatase genes encode pseudophosphatases. MTM pseudophosphatases bind active homologs and regulate the active enzyme's localization and enzymatic activity (Tonks, 2006). Loss of pseudophosphatase function in the MTM family has been implicated in the development of Charcot-Marie-Tooth (CMT) disease type 4B, a neuropathy with abnormal nerve myelination (Robinson and Dixon, 2005).

EGG-3, EGG-4 and EGG-5 are pseudophosphatases that have been characterized as necessary for the transition from oocyte to zygote in *C. elegans*. EGG-3, EGG-4 and EGG-5 are required to regulate MBK-2, a dual-specificity tyrosine kinase (DYRK) that phosphorylates substrates involved in the breakdown of microtubules, transcriptional silencing and polarization of the zygote (Tonks, 2009). EGG-3 binds the N-terminus of the kinase; EGG-4 and EGG-5 bind the activation loop (Cheng et al., 2009; Parry et al., 2009). EGG-4 and EGG-5 share 99% sequence similarity and are highly redundant, but loss of EGG-4 and EGG-5 leads to maternal effect lethality (Tonks, 2009).

MK-STYX

MK-STYX [MAPK (mitogen-activated protein kinase) phosphoserine/threonine/tyrosine-binding protein] is a pseudophosphatase of the DSP family and the subject of this thesis. MK-STYX is not catalytically active: at the

active site signature motif MK-STYX is missing the histidine and cysteine residues, and instead has phenylalanine and serine residues (FSX₅R) (Figure 2). A synthetic mutant in which the motif of MK-STYX was changed to the signature PTP active motif (HCX₅R) has the ability to dephosphorylate residues (Hinton et al., 2010). MK-STYX is structurally related to MKPs, and studies have identified MK-STYX in intriguing contexts; however mechanisms are not well elucidated. MK-STYX is highly expressed in Ewing's sarcoma family tumors (Siligan et al., 2005), and MK-STYX is a regulator of mitochondrial dependent apoptosis (Niemi et al., 2011). MK-STYX has also been identified to interact with G3BP-1 [Ras-GAP (GTPase-activating protein) SH3 (Src homology 3) domain-binding protein-1] and is implicated in the stress response pathway by decreasing stress granule formation (Hinton et. al, 2010).



Figure 2. MK-STYX diagram. MK-STYX has two N-terminal CH2 (Cdc25 homology 2) domains, CH2-A and CH2-B. MK-STYX is a pseudophosphatase due to the differences in the PTP signature motif. Instead of the active catalytic motif HCX₅R, MK-STYX has FSX₅R.

G3BP

The *Drosophila* homolog of G3BP (Ras-GTPase activating protein SH3 domain binding protein) was named Rasputin, because it has a position of power in cell signal transduction and its role is disputed, similar to Rasputin's role in Russian royalty (Irvine et al., 2004). Mammals have three G3BP proteins that are ubiquitously expressed: G3BP-1, 2a and 2b. G3BP plays a role in many cell functions, and is described as "promiscuous" because it is involved in many processes (Irvine et al., 2004). The N-terminus of G3BP has a nuclear transport factor (NTF) 2-like domain; G3BP can enter the nucleus, and acts as a DNA and RNA helicase (Costa et al., 1999). However, its localization is mostly cytoplasmic (Parker et al., 1996). G3BPs are also characterized by proline-rich regions and an RGG-box, which is a RNA binding recognition motif enriched by arginine and glycine. G3BP is an RNA-binding protein recruited to stress granules (Irvine et al., 2004). G3BPs bind the SH3 domain of RasGAP (Ras GTPase Activating Protein) (Parker et al., 1996). RasGAPs regulate Ras signaling by attenuating the active, GTP-bound state. RasGAP is important for Ras signaling independent of MAPK signaling (Tocque et al., 1997). Signaling involving the RasGAP SH3 domain has been implicated in oncogenic signaling pathways, cytoskeletal reorganization and cell adhesion (Leblanc et al., 1999; Leblanc et al., 1998).

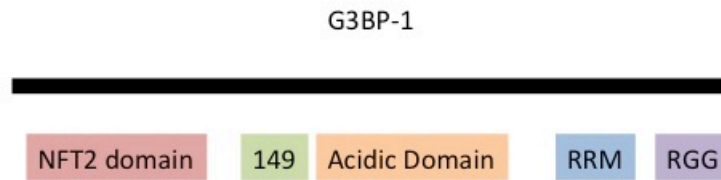


Figure 3. G3BP-1 Diagram. G3BP-1 has an N-terminal NFT2 (nuclear transport factor 2)-like domain that plays a role in nuclear localization. Serine 149 is a site of phosphorylation, and dephosphorylation at 149 allows for G3BP-1 aggregation and stress granule formation. Neighboring site 149 is an acidic domain. The RRM (RNA recognition motif) and RGG (arginine glycine rich) domains are important for RNA binding.

Stress Granule Formation

Stress granules are cytoplasmic storage sites for mRNA and play a key role in determining the fate of RNA during stress. Stress granules assemble in response to stressors such as heat shock, UV irradiation and hypoxia. Stress granules are non-membranous, range from 0.1 to 2.0 μm and rapidly aggregate (Anderson and Kedersha, 2009). They have been observed in yeast, protozoa and metazoans, including human cells, *C. elegans*, and in plants and in chloroplasts (Anderson and Kedersha, 2009).

In mammalian cells, stress granule formation is triggered by the phosphorylation of eIF2 α (eukaryotic initiation factor 2 alpha) (Kedersha et al, 1999, 2002). eIF2 has three subunits: alpha, beta, and gamma. Phosphorylation

of the alpha subunit on serine 51 prevents a GDP to GTP exchange on the gamma subunit. This exchange is mediated by a GTP exchange factor (GEF), eIF2B. The eIF2-GDP bound state is not able to bind transfer RNA and methionine, and thus phosphorylation of the alpha subunit prevents ternary complex formation necessary for translation of mRNA to protein. The stalled, translation pre-initiation complex, also referred to as the 48S pre-initiation complex, accumulates in cells to form stress granules. Generally, the presence of stress granules mirrors the increase in phosphorylation of eIF2 α (Kedersha and Anderson, 2002). Stress granules contain components of the stalled translation pre-initiation complex including phospho- eIF2 α , eIF3, eIF4E, eIF4G, and small ribosomal subunits (Kedersha et al., 2002). These initiation factors and the stalled 48S complex are considered the “core components” of stress granules.

There is a mechanism of stress granule formation independent of eIF2 α phosphorylation observed in non-mammalian cells, suggesting that mammals evolved an alternative mechanism to cope with stress (Farny et al., 2009). In *Drosophila*, stress granule assembly in response to heat shock is eIF2 α -phosphorylation independent (Farny et al., 2009). However, in mammalian cells, stress granule assembly in response to heat shock is dependent on eIF2 α phosphorylation (Farny et al., 2009). Also, drug inhibitors of eIF4A are able to trigger stress granule formation. eIF4A is a helicase that allows the translation initiation complex to scan mRNA for a start codon. Blocking eIF4A function can

promote stress granule assembly independently of eIF2 α phosphorylation (Farny et al., 2009).

Stress granules also contain other proteins that vary with cell type and the type of stress involved (Anderson and Kedersha, 2009). Proteins recruited to stress granules include transcription factors, nucleases, Argonaute proteins, microRNAs, mRNA-editing enzymes, kinases, and signaling molecules. The recruitment of signaling molecules, such as TRAF2 (TNF receptor associated factor 2), and RACK1 (receptor for activated C kinase 1) has been reported as a determinant of cell fate (Anderson and Kedersha, 2009). Other proteins involved in stress granule assembly include RNA-binding proteins TIA-1 (T-cell intercellular antigen 1), TIAR (TIA receptor), the PABP-1 (poly(A)⁺ binding protein), and HuR (human antigen R) (Kedersha et al., 1999). Research has suggested that these RNA-binding proteins, along with the initiation “core components” recruited to stress granules, are recruited as a complex due to similar kinetics of assembly and disassembly (Kedersha et al., 2000). TIA-1 is recruited to stress granules by binding stalled translation pre-initiation complexes, and this is dependent on a prion-like domain of TIA-1 (Gilks et al., 2004). Thus, stress granule assembly is triggered by eIF2 α phosphorylation and mediated by the aggregation of an RNA-binding protein such as TIA, Fragile X Mental Retardation Protein or G3BP (Gilks et al., 2004; Mazroui et al., 2002; Kedersha et al., 2005). Stress granule assembly is also dependent on microtubules (Thomas, et al., 2005).

As noted earlier, G3BP-1 is an RNA-binding protein that aggregates and mediates stress granule assembly; overexpression of G3BP-1 can dominantly induce stress granule assembly (Tourriere et al., 2003). Stress granules assembled in response to G3BP-1 overexpression are similar in composition with stress granules induced by stress; however, G3BP-1 induced stress granules are larger on average (Kedersha et al., 2005). Studies of G3BP-1 have revealed that the phosphorylation status of G3BP-1 at serine 149 is important for stress granule formation (Tourriere et al., 2003). Dephosphorylation of G3BP-1 at serine 149 causes G3BP-1 aggregation and stress granule formation (Tourriere et al., 2003). A phosphomimetic mutant (S149E) was used to demonstrate that a mutation from serine to glutamic acid at site 149, which mimics constitutive phosphorylation, fails to assemble stress granules (Tourriere et al., 2003). A non-phosphorylatable mutant (S149A) demonstrates that a mutation to alanine at site 149 causes G3BP oligomerization and stress granule assembly (Tourriere et al., 2003). Dephosphorylation of serine 149 can be induced by arsenite treatment, but also Ras signaling is implicated in stress granule assembly by regulating G3BP dephosphorylation.

Overexpression of G3BP-1 is implicated in the regulation of eIF2 α phosphorylation; G3BP-1 overexpression led to increased eIF2 α phosphorylation and knockdown of G3BP-1 led to reduced amounts of eIF2 α phosphorylation during recovery from stress (Wehner et al., 2010). The role of G3BP-1 in regulating eIF2 α phosphorylation is unclear and most likely not direct. G3BP-1

does not co-immunoprecipitate with eIF2 α ; however, G3BP-1 does interact with OGFOD1 (2-Oxoglutarate and Fe(II)-Dependent Oxygenase Domain Containing 1). OGFOD1 co-immunoprecipitates with eIF2 α (Wehner, 2010). OGFOD1 has been reported as a stress granule component that interacts with the ribosome and eIF2 α . Modulation of OGFOD1 abundance influences levels of phosphorylated eIF2 α in unstressed cells and cells recovering from arsenite-induced stress (Wehner, 2010).

Translation initiation

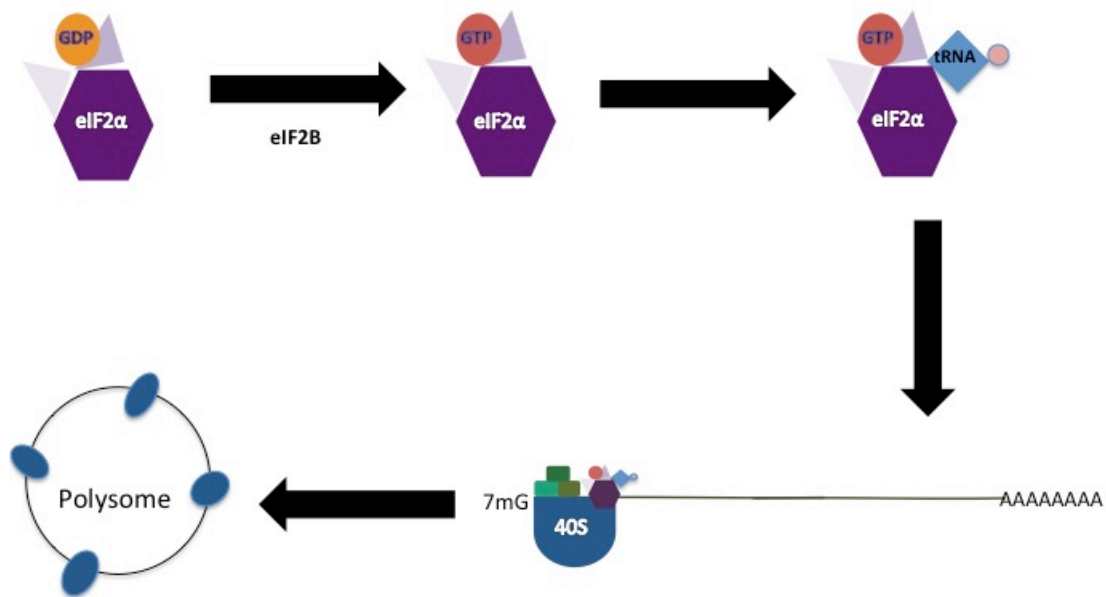


Figure 4. Translation initiation. For translation to be initiated, eIF2B is needed to exchange GDP for GTP on the gamma subunit of eIF2 α . This exchange allows

the translation initiation complex to form, which include eIF2 α -tRNA-Met. When this complex is available, the small ribosomal subunit (40S) and initiation factors comprise the 48S translation pre-initiation complex. The 48S complex assembles near the 5' end of the mRNA transcript and begins scanning for a start codon. Once a start codon is found, the large ribosomal subunit is recruited and translation can be initiated. Many ribosomes simultaneously translating one mRNA transcript comprise a polysome.

Translation inhibition

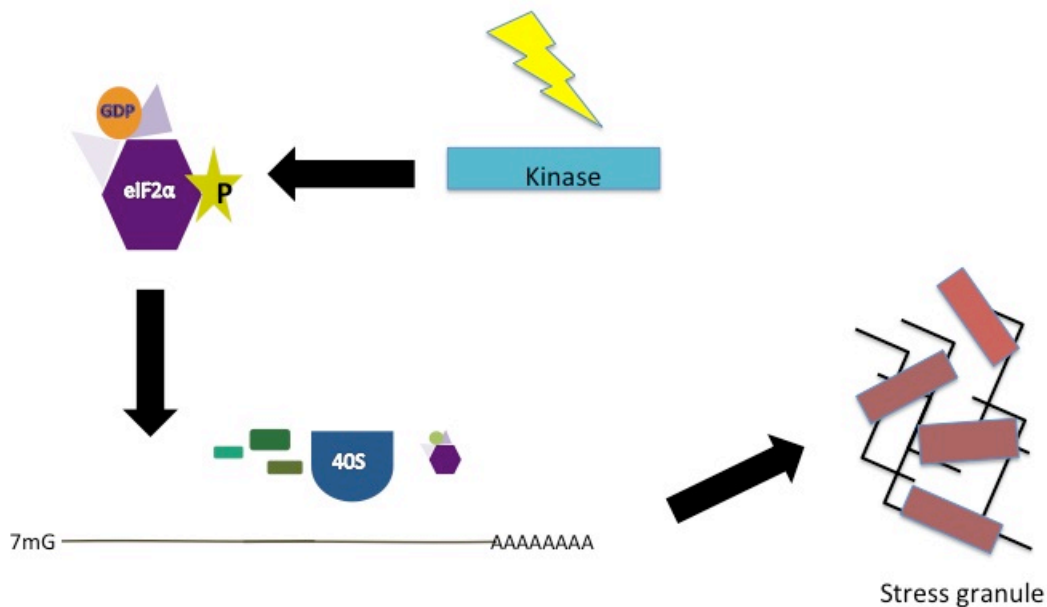


Figure 5. Translation inhibition by eIF2 α phosphorylation. During stress, eIF2 α is phosphorylated by a kinase on the alpha subunit. This phosphorylation event

inhibits eIF2B from exchanging GDP to GTP on the gamma subunit of eIF2 α . This prevents translation pre-initiation complex formation and inhibits general translation.

Eukaryotic Initiation Factor 2 Alpha (eIF2 α)

Multiple kinases and phosphatase complexes are known to regulate eIF2 α phosphorylation. The kinases include PERK (protein RNA-like endoplasmic reticulum kinase), which phosphorylates eIF2 α in response to endoplasmic reticulum stress; GCN2 (general control nonrepressed 2), which acts in response to amino acid deprivation; PKR (protein kinase R), which acts in the presence of double stranded RNA molecules; and HRI (heme-regulated inhibitor kinase), which acts during oxidative stress. Phosphorylation of eIF2 α and inhibition of general translation is a critical response to stress. Phosphorylation of eIF2 α is a cytoprotective mechanism; eIF2 α kinase inhibition has led to decreased cell survival, and inhibition of eIF2 α phosphatases has led to increased cell death. eIF2 is necessary for protein translation, which is a fundamental cellular process, and defects in eIF2 are lethal.

Misregulation of PERK activation and eIF2 α phosphorylation has been implicated in neurodegenerative diseases such as Alzheimer's, Parkinson's and Huntington's disease (Peel, 2004; Chang et al., 2002; Bando et al., 2005). In addition, mutations in eIF2B are implicated in vanishing white matter, a disease

in which minor traumas lead to major neurological deterioration and death (Bugianai, 2010). eIF2B is a GTP exchange factor (GEF) that activates translation by converting eIF2 from the GDP bound state to a GTP bound state.

The phosphatase known to regulate eIF2 α phosphorylation is PP1 (protein phosphatase 1). During stress, the PP1 regulatory subunit, GADD34 (growth arrest and DNA damage-inducible 34, also known by its gene name, *PPP1R15A*: protein phosphatase 1 regulatory subunit 15A), is selectively transcribed and binds the PP1 catalytic subunit to provide negative feedback for stress response (Wiseman and Kelly, 2011). A second PP1 regulatory subunit is known to regulate eIF2 α constitutively. CReP (constitutive repressor of eIF2 α phosphorylation, or *PPP1R15B*), binds the PP1 catalytic subunit to catalyze dephosphorylation of eIF2 α (Wiseman and Kelly, 2011). Knockout mice for both GADD34 and CReP leads to embryonic lethality, and this phenotype is rescued by mutation for a non-phosphorylatable eIF2 α mutant (Harding et al., 2009). This suggests that expression of GADD34 and CReP are essential processes. The lipid phosphatase PTEN (phosphatase and tensin homolog) has recently been implicated in the regulation of CReP and subsequent eIF2 α phosphorylation (Zeng et al., 2011). Inhibition of phosphatase complexes regulating eIF2 α phosphorylation delay translational recovery and lead to increased cell survival (Wiseman and Kelly, 2011). Cell signaling to maintain appropriate levels of eIF2 α phosphorylation is important in determining cell fate in response to stress.

Stress Granule Life Cycle

Observations from time-lapse microscopy indicate that an individual stress granule can have a life span of hours (Anderson and Kedersha, 2009). However, FRAP (fluorescence recovery after photobleaching) experiments show that RNA-binding proteins associated with stress granules are shuttling on the order of seconds and minutes (Anderson and Kedersha, 2009). The dynamic movement of stress granule components supports the theory that stress granules are sites of mRNA sorting and that they are not long-term bodies of the cytoplasm. Stress granule sorting decides whether mRNAs can be re-packaged for translation or degraded (Kedersha et al., 2000). It is suggested that stress granules shuttle mRNAs for degradation to processing bodies (P-bodies) (Kedersha et al., 2005). P-bodies are structurally similar to stress granules; however, they are distinct from stress granules and are sites of mRNA degradation. P-bodies contain components of the 5' to 3' mRNA degradation pathway. This pathway involves the removal of the 7-methyl guanosine cap from the 5' end of the transcript by the DCP-1/DCP-2 (mRNA decapping enzyme) complex, which is recruited to P-bodies (Kedersha et al., 2005).

Studies of stress granules imply that there is a dynamic equilibrium between stress granules and polysomes. Polysomes are sites of mRNA translation consisting of a cluster of ribosomes translating an mRNA molecule. Drugs that stabilize polysomes induce stress granule disassembly, and drugs

that dismantle polysomes cause stress granule assembly (Kedersha et al., 2002). Research suggests that stress granules are assembled due to stress that overloads polysomes with stalled initiation complexes. These complexes are then shuttled into stress granules rapidly, escorted by TIA-1. FRAP shows that 50% of stress granule-associated TIA-1 is replaced every two seconds (Anderson and Kedersha, 2002). Stress granule disassembly is mediated by Hsp70 (Kedersha and Anderson, 2002). Stress granule formation sequesters general mRNA; however, stress conditions allow for the translation of selective mRNAs for proteins aiding in stress response such as heat shock proteins (Hsps).

Heat Shock Response

The heat shock response is a conserved signaling pathway that is activated even by an increase of just a few degrees, and heat stress leads to the aggregation of proteins and imbalance of protein homeostasis. Cells do not recognize temperature change per se, instead the heat shock response is a response to the presence of unfolded proteins (Richter et al., 2010). Heat shock triggers stress granule formation in the cytosol, correlated with a decrease in global translation, which is described as a hallmark of the heat shock response (Ashburner and Bonner, 1979; Richter et al., 2010). Heat shock also disrupts the cytoskeleton, fragments the Golgi and endoplasmic reticulum, triggers the

formation of granules in the nucleus of stalled ribosomal assembly machinery, and leads to increased cell membrane permeability (Richter et al., 2010).

The heat shock response induces expression of heat shock proteins (Hsps) as a protective mechanism. Expression of Hsp chaperones is rapid in response to heat shock; this response is well characterized in yeast and takes 10 to 15 minutes (Richter et al., 2010). These molecular chaperones assist in protein folding and prevent aggregation. In the heat shock response, they recognize misfolded proteins by binding to exposed, hydrophobic amino acids that are sequestered when a protein is folded normally. By binding to the exposed, hydrophobic regions, the chaperones prevent protein aggregation. Hsp70 is a molecular chaperone that is not only a “holdase” of hydrophobic regions but also a “foldase” (Richter et al., 2010). Hsp70 is induced by stress, but Hsc70 is a constitutively expressed form that helps in protein folding under normal cell conditions.

Depending on duration and severity, heat shock can lead to cell death. However, if a cell survives heat stress, the response of Hsp expression can lead to a tolerance to stress and resistance (Richter et al., 2010).

MK-STYX and Stress Granules

As described earlier, MK-STYX decreases stress granule formation and is a binding partner of G3BP-1 (Hinton et al., 2010). In a prior study, G3BP-1

induced stress granules are dependent on dephosphorylation at serine 149 (Tourriere et al., 2003). G3BP-1 mutants were used to determine that the reduction of stress granules in the presence of MK-STYX is independent of G3BP-1 phosphorylation status. The mutant G3BP-S149A cannot be phosphorylated, and overexpression assembles stress granules. MK-STYX inhibits stress granule assembly induced by overexpression of G3BP-S149A, which suggests that MK-STYX regulates stress granule assembly independently of G3BP-1 phosphorylation (unpublished data). The mutant G3BP-S149E mimics constitutive phosphorylation and does not trigger stress granule assembly. A mutant of MK-STYX, which is a catalytically active phosphatase, leads to stress granule assembly with both G3BP-S149A and G3BP-S149E (unpublished data). This is unexpected because G3BP-1 induced stress granule assembly is dephosphorylation-dependent. This finding further implicates MK-STYX as a regulator of stress granule assembly induced by G3BP-1 overexpression.

Thesis objectives

The overall aim of this thesis was to investigate the effect of MK-SYX on stress granule assembly and disassembly by examining the interactions between MK-STYX, eIF2 α , and Hsp70 (Figure 6). A foundation for further characterization of MK-STYX functions using bioinformatics, localization studies and microarray was laid.

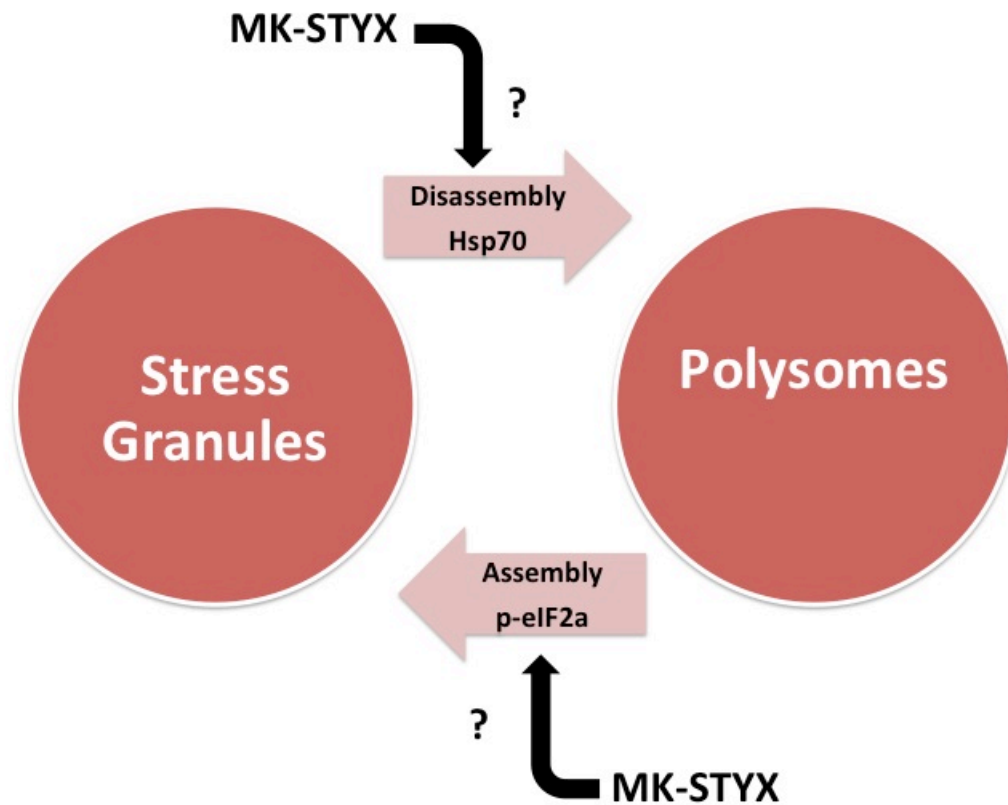


Figure 6. Investigation of MK-STYX stress granule reduction. MK-STYX could enhance stress granule disassembly, which is mediated by Hsp70. Alternatively, MK-STYX could inhibit stress granule assembly, which is initiated by phosphorylation of eIF2 α .

METHODS

Plasmids

pMT2-FLAG-MK-STYX-FLAG was constructed as described in Hinton et al., 2010. The N-terminal and C-terminal ends of human MK-STYX are flanked by the FLAG epitope for MK-STYX detection. The integrity of the construct was confirmed by sequencing.

G3BP-GFP, G3BP1-149A-GFP and G3BP1-149E-GFP constructs were provided as a gift by Dr. Jamai Tazi of the Institut de Génétique Moléculaire, France.

Cell Culture, Transfection, and Heat Shock

All experiments used HeLa cells (ATCC CCL-2), which are human cervix epithelioid carcinoma cells. HeLa cells were grown at 37°C and 5% CO₂ in Minimal Essential Medium (Gibco, Invitrogen) supplemented with 10% fetal bovine serum (Invitrogen). Transient transfection of HeLa cells was performed using 4 µl Lipofectamine 2000 Reagent per µg DNA (Invitrogen). For all transfections, cell media was removed and replaced 5 hours following transfection. Cells were stressed by heat shock of 41°C for 1 hour, 23 hours post-transfection. Cells were immediately fixed or lysed afterward.

For harvesting cell lysate, HeLa cells were seeded on 10 cm dishes, transfected with 4 µg DNA and lysed forty-eight hours post-transfection using lysis buffer (50 mM HEPES, pH7.2; 150 mM NaCl; 10% glycerol; 10 mM NaF; 1% Nonidet P-40 alternative [Calbiochem] and protease inhibitor cocktail tablets [Roche]).

Cell Imaging

For cell imaging, 2 x 10⁵ cells were grown in 6-well plates with coverslips. Cells in each well were transfected with a total of 2 µg DNA 24 hours after plating at 40 to 60 percent confluence. Twenty-four hours post-transfection cells were washed

with PBS and fixed with 3.7% formaldehyde, and the coverslips were mounted to slides using Fluoro Gel II, with DAPI (4', 6-diamidino-2'-phenylindole dihydrochloride) (Electron Microscopy Sciences). Cells were analyzed using fluorescence microscopy.

Immunoblotting

Lysates were sonicated and centrifuged at 14,000 x g for 15 min. Protein concentration was determined using NanoDrop quantification. Lysate samples were boiled with sample buffer and dithiothreitol (DTT) and proteins were separated by 10% SDS-PAGE for 1 hour and 150 V. Protein gels were transferred to a PVDF membrane (GE Healthcare) using I-Blot (Invitrogen) or Trans-Blot Semi-Dry Transfer Cell (BioRad). Proteins were immunoblotted with anti-FLAG (Sigma), anti- β -tubulin (Thermo Scientific), anti-eIF2 α (Abcam), anti-phospho-eIF2 α (Abcam), and anti-Hsp70 (Cell Signaling) and in 5 percent milk-TTBS (Tris Buffer Tween20) or bovine serum albumin (Sigma). Protein bands were detected with enhanced chemiluminescence (ECL) or ECL Plus (GE Healthcare). Blots testing the effect of MK-STYX on phospho-eIF2 α were probed first with anti-phospho-eIF2 α (made in rabbit), then stripped and reprobed with anti-eIF2 α (made in mouse) and anti- β -tubulin.

Immunoprecipitation

Lysates were sonicated and centrifuged at 14,000 x g for 15 min. Protein concentration was determined using NanoDrop quantification. Lysates were pre-cleared with Protein G Beads (GE Healthcare). Next, the lysates were incubated for 1 hour at 4° C with anti-eIF2 α (Abcam), and then incubated 2 hours with Protein G Beads for pull-down. Samples were washed four times with lysis buffer and boiled with sample buffer and DTT. Proteins were separated by 10% SDS-PAGE for 1 hour and 150 V. Protein gels were transferred to a PVDF membrane (GE Healthcare) using i-Blot. Membranes were immunoblotted with anti-FLAG (Sigma).

BLAST

Basic local alignment search tool (BLAST) is a database available online from the National Center for Biotechnology Information (NCBI). This database is used to align and compare sequences. Protein BLAST was used to search for proteins with similar sequence to MK-STYX. Proteins were ranked by E-values, which are probability scores. E-values of e^{-50} or lower are considered a virtually identical sequence, and low E-values are most significant.

I-TASSER and StarBiochem

I-TASSER, the Iterative Threading Assembly Refinement Server, is the best software for protein structure prediction, according to 2006-2010 Critical Assessment of Structure Prediction experiments. It is a free, online server that builds 3D protein models based on multiple threading alignments. First, I-TASSER finds nonredundant sequences by position specific iterated BLAST (PSI-BLAST) to identify homologs, predict secondary structures and create a sequence profile. The sequence profile goes through threading; threading is a method where the computer program forces the sequence to adopt every known protein fold, and then scores the sequence's suitability for that fold. Existing protein folds are available in the Protein Data Bank (PDB) library. The score for sequence suitability for a protein fold is called a Z-score. I-TASSER next assembles the 3D structure. However, sequences without similarity to folds in the Protein Data Bank (PDB) library are modeled *ab initio*. I-TASSER also works to help predict protein function by matching ligand-binding sites with other known proteins. A confidence score, or C-score, is assigned to each structure and functional assertions. A C-score is in the range of (-5, 2) and a higher score means a better model structure. A protocol for interpreting I-TASSER results was published by Nature and used to for analysis (Roy et al., 2010).

The models generated by I-TASSER can be downloaded but the format requires a program that can open a .pdb file, such as StarBiochem. StarBiochem is a

molecular visualization program created by MIT, and allows users to interact with any PDB files.

Microarray

The 3DNA Array 350 Labeling Kit (Genisphere) was used for oligonucleotide cDNA detection. The microarray chip used was a Discover Chip (Array It). The chip has 380 different gene sequences. Each gene has 2 spots on the microarray for cDNA oligonucleotides hybridization. The chip has 4 grids, each grid has 14 rows and 14 columns.

Process overview: RNA was reverse transcribed with unlabeled dNTPs to cDNA with an RT primer provided by the kit. A 3DNA Capture Sequence provided by the kit was added that hybridizes with the 5' end of the RT primer. The cDNA, RT Primer, and 3DNA Capture Sequence were hybridized to the microarray Discover Chip. 3DNA Capture Reagent was added and binds cDNA on the microarray and contains the fluorescent signal, which can be scanned and analyzed.

In this experiment, lysates were harvested from 10 cm plates transfected with pMT2 and MK-STYX. RNA was isolated using Aurum Total RNA Mini Kit (Bio-Rad). 3 μ g of RNA present in pMT2 lysate was labeled with Cy3/AlexaFluor 546 RT Primer (green), and 3 μ g of RNA present in MK-STYX lysate was labeled with Cy5/AlexaFluor 647 RT Primer (red). The RNA-RT primer mixes were hybridized at 80° C for 10 minutes and put on ice directly afterward for 3 minutes. The hybridized RNA-RT primer mixes were added to a reaction mix for cDNA production, including 5X Superscript First Strand Buffer, dTT, dNTPs, RNase Inhibitor and Superscript II. The reaction mixes were incubated at 42° C for 2 hours. To end the reaction, 0.5 mM NaOH/50 mM EDTA was used.

The cDNA was concentrated using 3M Ammonium Acetate. The cDNA was incubated at -20° C for 30 minutes and centrifuged at 10,000 x g for 15 minutes. The supernatant was removed and the cDNA pellet was dried by heating for 30 minutes at 65° C. The cDNA pellet was resuspended in Nuclease Free Water and added to a cDNA Hybridization Mix including LNA dT Blocker, Nuclease Free

Water and Enhanced Hybridization Buffer. The cDNA Hybridization Mix was incubated at 75° C for 10 minutes and then at 60°C. The cDNA Hybridization Mix was pipetted onto the microarray and incubated overnight at 60°C in humidity and the dark.

The array was washed with 2X SSC, 0.2 percent SDS pre-warmed to 42°C, and 2X SSC and 0.2X SSC at room temperature. The array was dried by centrifugation at 1000 RPM for 2 minutes. The array was next hybridized with 3DNA Capture Reagent for both Cy3 and Cy5 RT Primer Capture Sequences. The 3DNA Hybridization Mix contained a Cy3 3DNA Capture Reagent, Cy5 3DNA Capture Reagent, Nuclease Free Water and Hybridization Buffer including Anti-Fade Reagent. The 3DNA Hybridization Mix was heated to 75° C for 10 minutes and applied to the array. The array was incubated for 3 hours at 60°C in humidity and the dark.

The array was washed and dried the same as after cDNA hybridization. The microarray was scanned using Gene Pix Personal 4100A Scanner (Molecular Devices). Microarray analysis used Magic Tool software, Adobe Photoshop and Image J.

Subcloning: MK_STYX-Cherry

PCR (Polymerase Chain Reaction) was used to amplify MK-STYX and MK-STYX Active Mutant. PCR Product Purification Qiagen Kit was used to purify amplified DNA. The Vector (mCherry) DNA and Insert (MK-STYX or MK-STYX Active Mutant) DNA were double digested by restriction endonucleases EcoR1 (New England BioLabs) and Xba1 (New England BioLabs) at 37°C on a hot plate for 3 hours. Double digestion with these two restriction enzymes is not recommended; however, double digestions was found to be more successful than sequential digestion by trial and error. The double digestion reactions were purified using PCR Product Purification (Qiagen). The ligation reaction requires T4 Ligase and Buffer, 100 ng of plasmid DNA, and a 3:1 ratio of insert to vector was determined most successful. DH5α competent cells were transformed on LB-agar plates with

kanamycin to screen colonies. Colonies were picked and specific primers were used to amplify MK-STYX and MK-STYX active mutant. Colonies that screened positive were picked and cultured overnight in LB. A mini-prep kit by Qiagen was used to purify the plasmid. Double digestion of the plasmid with EcoR1 and Xba1 was used to confirm the presence of insert. A further confirmatory step of PCR of the plasmid to amplify insert is currently underway.

RESULTS

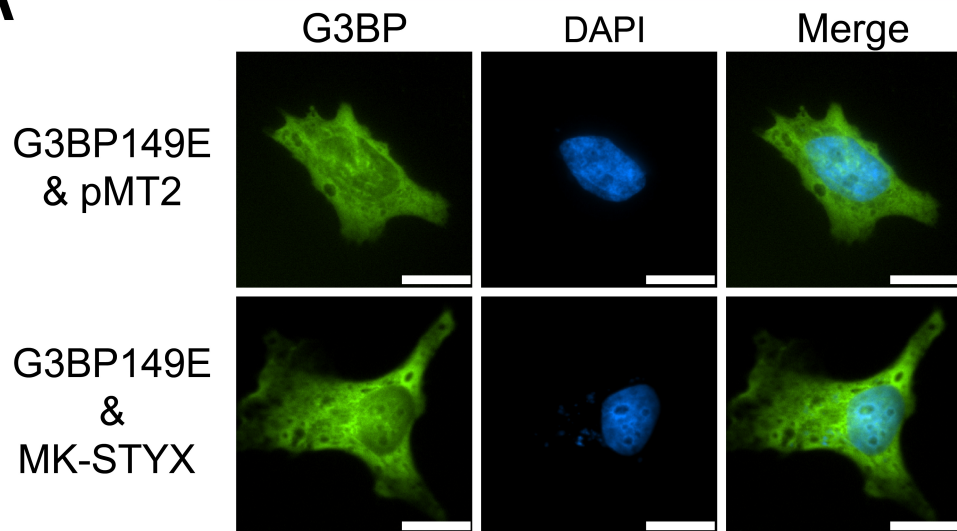
MK-STYX attenuates stress granule formation independently of G3BP-1 phosphorylation status

Many stressors induce stress granule assembly, including overexpression of G3BP-1; however, MK-STYX inhibits stress granule assembly (Hinton et al., 2010). G3BP-1 is regulated by phosphorylation events at serines 149 and 232, and dephosphorylation of G3BP-1 at site 149 has been implicated as necessary for stress granule assembly triggered by G3BP-1 overexpression (Tourriere et al., 2003). Since MK-STYX is a binding partner of G3BP-1, the effect of MK-STYX on stress granule assembly with varying states of G3BP-1 phosphorylation was determined.

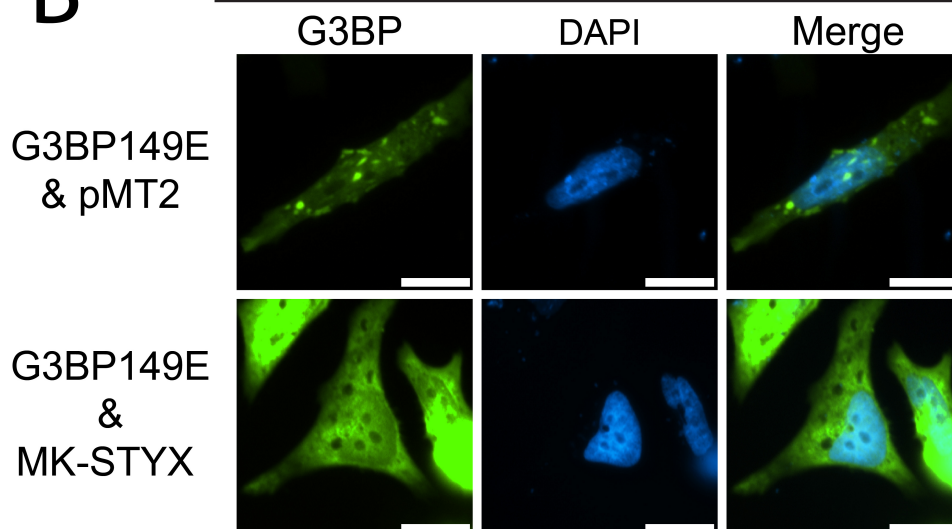
A phosphomimetic mutant, G3BPS149E, substitutes glutamic acid for serine at residue 149, and mimics constitutive phosphorylation. Under normal cellular conditions, this mutant, as expected, did not induce stress granule formation (Figure 7). However, under heat shock conditions, stress granules were assembled and G3BPS149E aggregated. Co-expression of MK-STYX and G3BPS149E under heat shock conditions attenuated stress granule formation (Figure 7). These results suggest that MK-STYX acts independently of G3BP-1 phosphorylation status to decrease stress granule formation.

A

No Heat Shock

**B**

Heat Shock



C

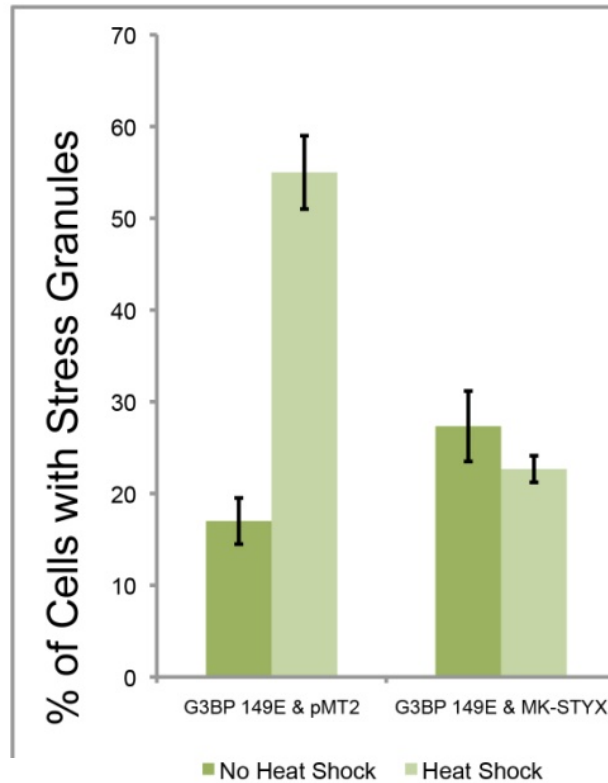


Figure 7. MK-STYX reduces stress granules induced by overexpression of the phosphomimetic mutant G3BP1-149E and heat shock. Cells were transiently transfected with constructs G3BP1-149E, MK-STYX or pMT2. pMT2 is a control because MK-STYX is transfected in a pMT2 plasmid vector. (A) Cells overexpressed with the G3BP1-149E phosphomimetic mutant do not assemble stress granules. (B) Cells overexpressed with G3BP1-149E assemble stress granules after heat shock. These stress granules are inhibited by co-expression of MK-STYX. (C) Heat shock induces stress granules in cells overexpressing G3BP 149E phosphomimetic mutant. Co-expression with MK-STYX decreases the formation of these stress granules.

MK-STYX decreases eIF2 α phosphorylation and interacts with eIF2 α

Phosphorylation of eIF2 α halts translation and triggers the disassembly of polysomes and the formation of stress granules (Farny, 2009). To determine if MK-STYX has an affect on the phosphorylation status of eIF2 α , western blotting was used. Western blotting shows that heat shock increases phosphorylation of eIF2 α (Figure 8). First, phospho-eIF2 α was blotted for with an anti-phospho-eIF2 α antibody, then the membrane was stripped and total eIF2 α protein levels were blotted for using an anti- eIF2 α antibody (Figure 8). In the presence of MK-STYX, phosphorylation of eIF2 α was reduced under basal conditions and subtly reduced during heat shock conditions (Figure 8). Co-immunoprecipitation results show that MK-STYX interacts with eIF2 α (Figure 8).

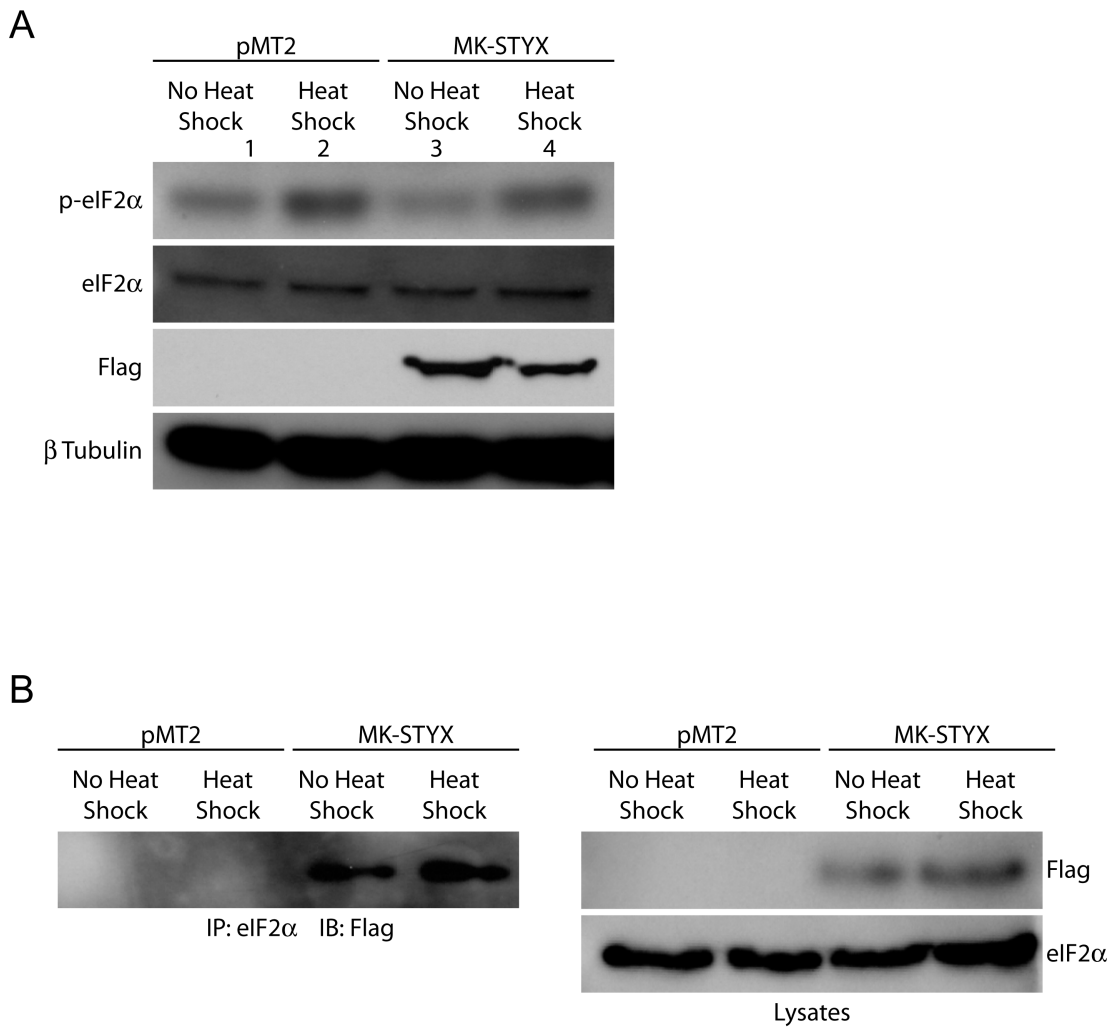


Figure 8. MK-STYX decreases eIF2 α phosphorylation and interacts with eIF2 α .

(A) Blotting of lysates for phosphorylated eIF2 α (n=3). Heat shock shows an increase in phosphorylated eIF2 α . The presence of MK-STYX displays a subtle decrease in phospho- eIF2 α compared to cell lysates transfected with the control, pMT2. Blotting for total eIF2 α protein levels shows a consistent level of eIF2 α among lysate. Blotting for tubulin is also a control to demonstrate consistent protein level among lysate. Blotting for flag shows detection of MK-STYX. (B) eIF2 α was immunoprecipitated (IP) from cell lysate, and blotting (IB) for flag shows detection of MK-STYX, indicating that eIF2 α and MK-STYX interact. Lysates show detection of MK-STYX and eIF2 α .

MK-STYX increases Hsp70 expression

To determine if MK-STYX has an affect on Hsp70, lysates were blotted for Hsp70 detection (Figure 9). The same membrane was used to blot for β -tubulin to demonstrate a consistent protein level across lysates. The presence of MK-STYX was detected using α -Flag on a separate membrane. These findings suggest that MK-STYX increases the expression of Hsp70, and important protein for stress granule disassembly.

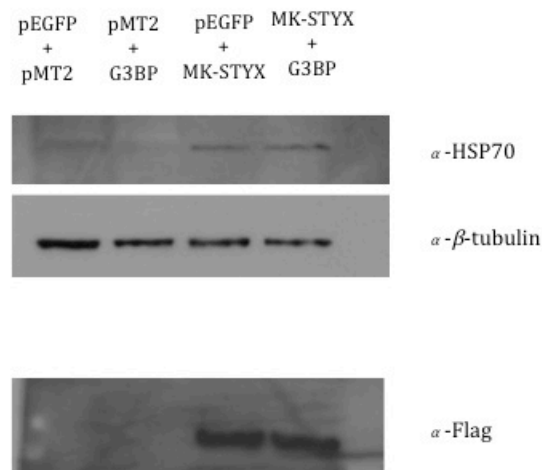


Figure 9. MK-STYX increases Hsp70 expression (n=2). Cells were transfected with pMT2, MK-STYX, pEGFP, and G3BP-1. pEGFP is a control for G3BP-1, because G3BP-1 resides in a pEGFP plasmid vector. This vector fluoresces green. Hsp70 levels were blotted for and display an increase in Hsp70 levels when MK-STYX is present. Tubulin was used as a control to show consistent protein levels among lysate. Flag was used to detect MK-STYX.

Sequence comparisons: BLAST

MK-STYX amino acid sequence: FASTA format

```
>sp|Q9Y6J8|STYL1_HUMAN Serine/threonine/tyrosine-interacting-like protein 1
OS=Homo sapiens GN=STYXL1 PE=2 SV=1
MPGLLLCEPTELYNILNQATKLSRLTDPNYLCLLDVRSKWEDSHVITALRVKKNNEY
LLPESVDLECVKYCVVYDNNSSSTLEILLKDDDDSDSDGDGKDLVPPQAAIEYGRILTRLT
HHPVYILKGGYERFSGTYHFLRTQKIIWMPQELDAFQPYPIEIVPGKVFVGNFSQACDPK
IQKDLKIKAHVNVSMDTGPFAGDADKLLHIRIEDSPEAQILPFLRHMCHFIEIHHHLGS
VILIFSTQGISRSCAAIIAYLMHSNEQTLQRSWAYVKKCKNNMCPNRLVLSQLLEWEKTI
LGDSITNIMDPLY
```

To determine proteins with similar sequence to MK-STYX, BLAST was used. In a BLAST human protein search, MKP-1 (shown as dual specificity phosphatase 1) is the most significant alignment besides other entries and

isoforms of MK-STYX, the E-value is $2e-16$. BLAST protein alignment between MK-STYX and MKP-1 has high query coverage of 86 percent (Table 1). However, the maximum identity is only 25 percent, and does not pass the “40 percent rule”. The “40 percent rule” allows for function to be inferred from sequence: if a protein has more than 40 percent sequence identity to another protein whose biochemical function is known, then a working assumption should be that these two proteins have a common biochemical function (Petsko and Ringe, 2004).

Accession	Description	Max Score	Total Score	Query Coverage	E value	Max Ident
NP_004408.1	dual specificity protein phosphatase 1	74.7	74.7	86	2.00E-16	25
NP_004409.1	dual specificity protein phosphatase 2	70.1	70.1	59	8.00E-15	28
NP_004410.3	dual specificity protein phosphatase 5	70.1	70.1	56	1.00E-14	30
AAH42101.1	dual specificity protein phosphatase 16	69.7	69.7	85	2.00E-14	25
NP_476499.1	Dual specificity phosphatase, isoform 2	63.5	63.5	56	1.00E-12	27

Table 1. Top 5 Non-redundant BLAST Results (query protein sequence is MK-STYX)

Comparing the two CH2 domains of MK-STYX and MKP-1 demonstrates sequence similarity (Wishart and Dixon, 1998). However, MK-STYX lacks the three arginines at residues 54, 55, and 56 that MKP-1 has (Figure 10). These three arginines are believed to be responsible for recognition of MAPKs and are boxed in red in Figure 10. Repeated arginines are thought to be a kinase interaction motif (KIM) conserved among MAPK phosphatases (Owens and Keyse, 2007). These arginines are believed to determine MKP-1 specific binding with p38 and ERK (Owens and Keyse, 2007). The BLAST sequence alignment between MK-STYX and MKP-1 shows that MK-STYX only has one arginine, and

has valine and lysines. Arginine and lysine are both positively charged amino acids, so this substitution may not be critical; however, this difference indicates that MK-STYX and MKP-1 may interact with different proteins. A second motif comprising of arginine at residues 72 and 74 has been recognized as necessary for MKP-1 to interact with JNK (Owens and Keyse, 2007). The arginine residues of this second motif do not align with MK-STYX.

MK-STYX and MKP-1 Sequence Alignment (Query Protein is MK-STYX, Subject is MKP-1)

```

GENE ID: 1843 DUSP1 | dual specificity phosphatase 1 [Homo sapiens]
(Over 100 PubMed links)

Score = 74.7 bits (182), Expect = 2e-16, Method: Compositional matrix adjust.
Identities = 76/301 (25%), Positives = 131/301 (44%), Gaps = 43/301 (14%)

Query 33 LLDVRSKWEYDESHVI-----TALRVKKKNN---EYLLPESVDLECVMKYCVVYDNNS 81
          LLD RS ++ H+          T +R + K          E+++P + +L          Y
Sbjct 26 LLDCRSFFAFNAGHIAGSVNVRVSTIVRRRAKGAMGLEHIVPNA-ELRGRLLAGAYH--- 81

Query 82 STLEILLKDDDDSDSDGDKLVPQAAIEYGRILTRLTHHPVYILKGGYERFSGTYHFL 141
          +LL D+ + DG +D          A+ G +          V+ LKGGYE FS + L
Sbjct 82 --AVVLL--DERSAALDGAKRD--GTLALAAGALCREARAAQVFFLKGGYEAFFSASCP 135

Query 142 RTQKIWM-----PQELDAF-----QPYPIEIVPGKVFVGNFSQACDPKI 181
          +++ M          P ++          Q P+EI+P +++G+ A +
Sbjct 136 CSKQSTPMGLSLPLSTSVFDSAESGCSSCSTPLYDQGGPVEILP-FLYLGSAHASRKDM 194

Query 182 QKDLKIKAHVNVSMDTGFFAGDADKLLHIRIEDSPEAQILPFLRHMCHFIEIHHHLGVS 241
          L I A +NVS + F G + I +ED+ +A I +          FI+ + G
Sbjct 195 LDALGITALINVSANCPNHFEHGY-QYKSIPVEDNHKADISSWFNEAIDFIDSIGNAGGR 253

Query 242 ILIFSTQGISRSCAAIIAYLMHSNEQTLQRSWAYVKKCKNNMCPNRLVLSQLEWEKTIL 301
          + + GISRS +AYLM +N L ++ +VK+ ++ + PN + QLL++E +L
Sbjct 254 VFVHCQAGISRSATICLAYLMRTNRVKLDEAFEFVKQRRSIIISPNSFMGQLLQFESQVL 313

Query 302 G 302
Sbjct 314 A 314

```

Figure 10. MK-STYX and MKP-1 Alignment. In the red box is the alignment region for the three repeated arginines of the KIM motif of MKP-1. MK-STYX has one arginine that aligns. MK-STYX does not have any repeated arginines in its sequence.

Structural Comparisons: I-TASSER

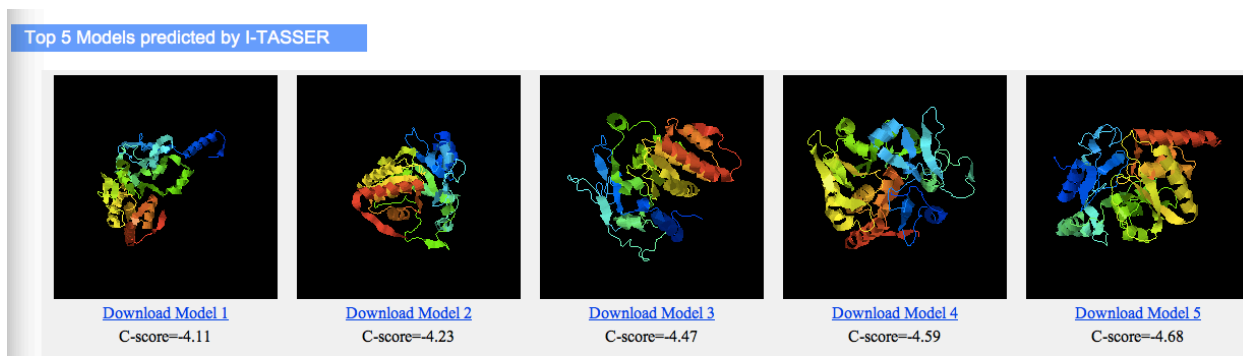


Figure 11. MK-STYX structure models predicted by I-TASSER. 5 structural models were created by I-TASSER and confidence scores given for each model. Confidence scores range from -5 to 2, with 2 being the most confident. Model 1 is the best model because it has the highest C-score of -4.11.

To determine the predicted structure of MK-STYX, I-TASSER was used. I-TASSER gave five predicted structures, all with C-scores less than -4 (Figure 11). C-scores are calculated based on threading alignments, and a C-score greater than -1.5 generally has a correct fold. Therefore, much confidence cannot be given to these models.

The top ten threading templates are identified, and in this run there is redundancy of templates used. The top ten templates from the PDB library that are not redundant are: mouse dual specificity phosphatase, human dual specificity phosphatase 5, human dual specificity phosphatase 27, human dual specificity phosphatase 14, the catalytic domain of human MKP-5, and human dual specificity phosphatase 18. The normalized Z-score can be used to analyze the quality of threading alignment. An alignment with a normalized score of Z greater than 1 means a correct alignment. All of the top ten templates used by I-TASSER have a normalized Z-score greater than 1.

Coverage is the number of aligned residues divided by the length of the query protein. Coverage for the templates used is low. Therefore, the high, normalized-Z score is not accurate for the full-length query protein, and is only accurate for the aligned regions. All alignments occurred between residues 160 to 300. This indicates a better alignment for the region of the MK-STYX protein with the PTP motif, and not the N-terminal CH2 domains.

Top 10 Identified structural analogs in PDB

Rank	PDB Hit	TM-score	RMSD ^a	IDEN ^a	Cov.	Download Alignment
1	2y96A	0.524	1.15	0.208	0.537	Download
2	2qwoC	0.468	1.74	0.198	0.489	Download
3	2hcmA	0.466	1.97	0.255	0.502	Download
4	1vhrA	0.464	1.70	0.195	0.486	Download
5	1g4wR	0.462	3.88	0.083	0.572	Download
6	1zvrA2	0.455	3.96	0.047	0.566	Download
7	1lw3A	0.455	3.97	0.034	0.566	Download
8	2oudA	0.454	2.23	0.247	0.486	Download
9	2yf0A	0.447	4.06	0.040	0.562	Download
10	2wgpA	0.445	1.72	0.219	0.467	Download

1. Human dual specificity phosphatase 27
2. Human TMDP
3. Mouse dual specificity phosphatase
4. Human VH1-related dual specificity phosphatase
5. SPTP
6. MTMR2
7. MTMR2
8. Catalytic domain human MKP-5
9. MTMR6
10. Human dual specificity phosphatase 14

Table 2. Structural analogs of MK-STYX generated by I-TASSER. Table 2 shows the structural analogs identified from the PDB library. Structural analogs are based on TM-align, which is an algorithm that compares two proteins that can have different sequences, and considers residues equivalent based on structure. The TM-score generated from TM-align greater than 0.5 indicates the structures have the same fold. Again, coverage is limited. The identity column is sequence identity in the structurally aligned regions, and RMSD measures conserved spatial motifs between structures.

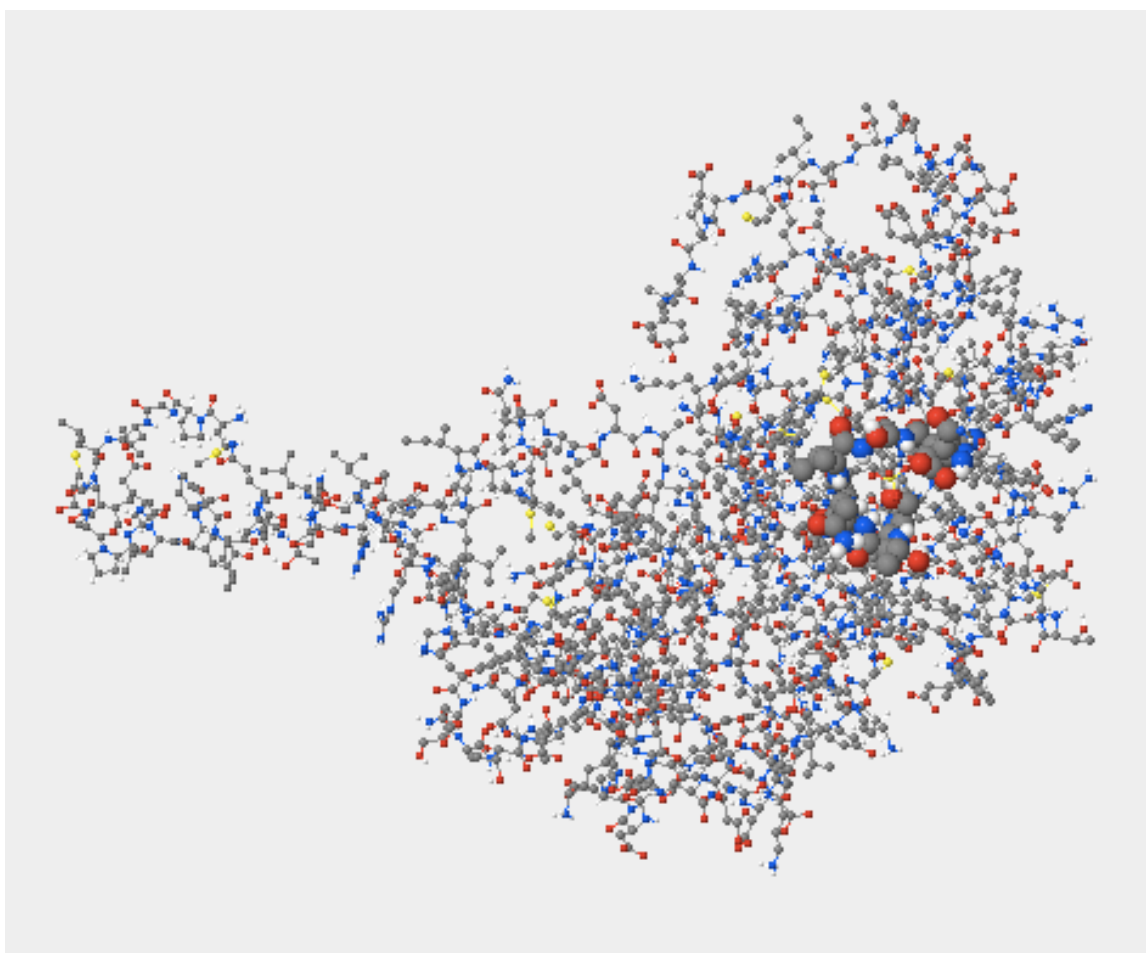


Figure 12. MK-STYX model by I-TASSER and predicted binding site. The model of MK-STYX with the highest C-score was opened visualized using a ball and stick model in StarBiochem. The predicted binding site residues were enlarged.

I-TASSER predicts function by identifying a predicted binding site through comparisons to template binding sites. The template protein with the most similar binding site was MKP-5. MK-STYX residues predicted to be a binding site for protein interactions are aspartate 215, serine 246, threonine 247, glutamine 248, glycine 249, isoleucine 250, serine 251, and arginine 252 (D...SX₅R). The MK-STYX model was downloaded into Star Biochem and the binding site residues enlarged for visualization (Figure 12). The predicted binding site by I-TASSER

corresponds with the conserved PTP motif that is catalytically inactive in MK-STYX. This suggests that this region of MK-STYX, despite catalytic residues, retains a fold like the PTP domain of active homologs.

Microarray

To determine affects of MK-STYX on gene expression microarray was used. The microarray scan showed fluorescence and could be analyzed using Magic Tool. The microarray red and green images were overlaid and gridded (Figure 13). The gene list was imported into Magic Tool so spots can be identified.

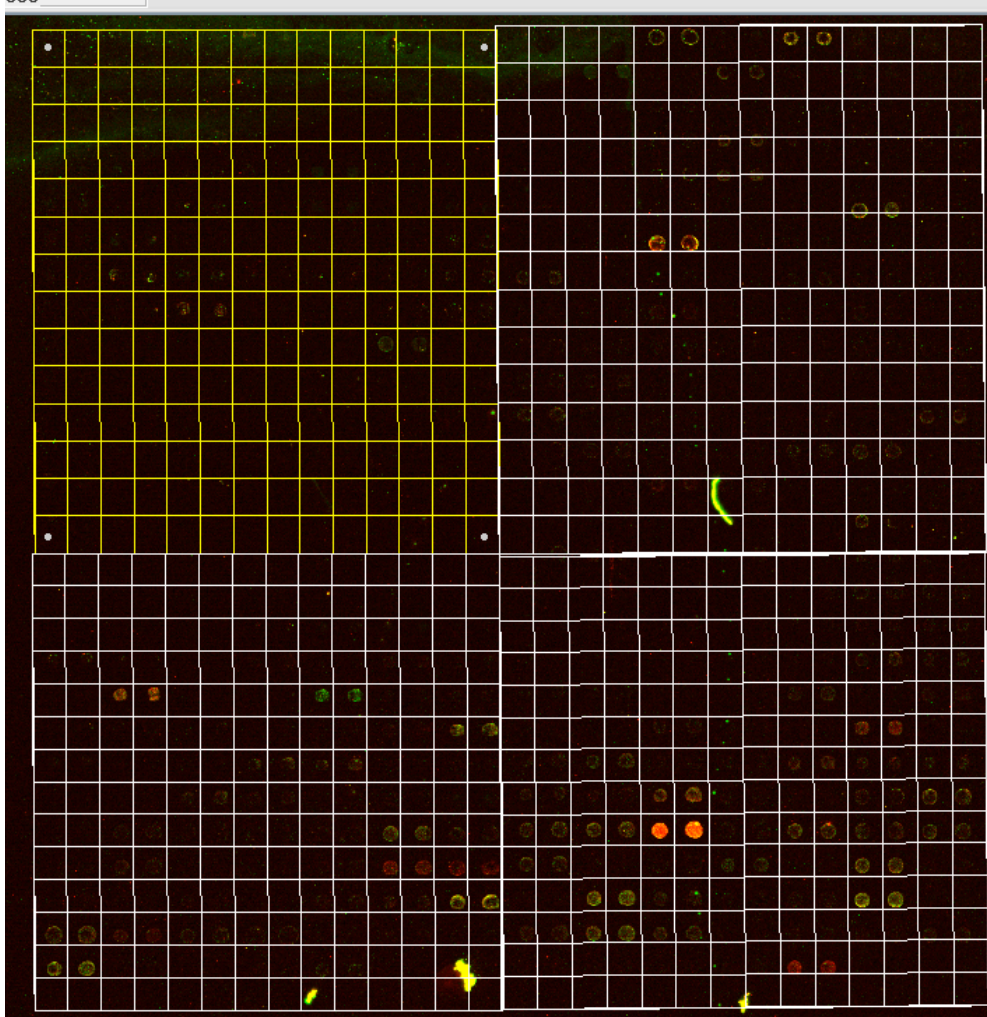


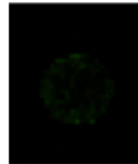
Figure 13. Microarray grid. Both red and green fluorescent scans were overlaid and the spots were gridded using Magic Tool. Gridding allows for identification of

genes by corresponding quadrants, rows and column numbers with the gene list for the Discovery Chip.

Red spots indicate greater hybridization of cDNA from lysate of cells transfected with MK-STYX. Green spots indicate greater hybridization of cDNA from lysate of cells transfected with pMT2. Yellow spots indicate hybridization of cDNA from both MK-STYX and pMT2 transfected cell lysate. Two spots in the fourth quadrant stand out in orange and indicate cDNA hybridization with PCTAIRE Kinase 1. This suggests greater expression of the PCTAIRE Kinase 1 gene in the presence of MK-STYX.

Color Hisotgram Analysis of Spot 1: **546**

Count	864
rMean	0
rSD	0
rMode	0
gMean	3.37
gSD	6.34
gMode	1
bMean	0
bSD	0
bMode	0



Color Histogram Analysis of Spot 1: **647**

Count	924
rMean	24.05
rSD	44.21
rMode	4
gMean	0
gSD	0
gMode	0
bMean	0
bSD	0
bMode	0

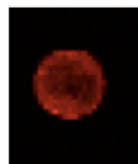


Figure 14. PCTAIRE Kinase 1, Spot 1 Analysis. The scan for the green wavelength (546) was compared for the scan for the red wavelength (647) of the same spot. Analysis by Image J shows a difference in pixels detected for the

scans, suggesting a difference in gene expression between control and MK-STYX transfected cell lysate.

To quantify the difference between the green fluorescence and red fluorescence Magic Tool was not ideal. Adobe Photoshop was used to open images from the microarray scan and Image J was used to analyze a spot to demonstrate a difference in expression. Image J is an analysis program created by the National Institutes of Health. There are two spots for PCTAIRE Kinase 1; Spot 1 was analyzed and is on Quadrant 4, Column 5, Row 9 of the microarray chip. This is a simple demonstration of the difference between the green (wavelength 546) label for pMT2 expression and red (wavelength 647) for MK-STYX expression. A color histogram analysis showing colors present and amount detected was conducted using Image J for spot 1 (Figure 14). Another analysis using image J was a gray scale to compare pixels of spot 1 from the green fluorescence scan and the scan for red fluorescence (Table 3).

	Area	Mean	Min	Max	IntDent	RawIntDent
Grayscale 647	7.80E-04	9.21	0	105	0.007	7184
Grayscale 546	8.64E-04	2.337	0	27	0.002	2019

Table 3. Grayscale comparison of PCTAIRE Kinase 1, Spot 1. This is another comparison of Spot 1 546 and Spot 1 647. This standardizes for comparison of minimum and maximum gray values, mean gray value, and integrated density. Integrated density is the product of area and mean gray value. The raw integrated density is the sum of the values of pixels in the selection.

Taken together, this data implies that MK-STYX has an effect on gene expression in the cells, indicating that MK-STYX plays a role in the cell. Other genes that were also noticeably highly expressed in cell lysate transfected with

MK-STYX include cyclin dependent kinase inhibitor 1A (CDK 1A, p21), pyruvate dehydrogenase (lipoamide) alpha 1, v-akt murine thymoma viral oncogene homolog 1, glucocorticoid receptor DNA binding factor 1, MKP-3, and proteoglycan 3. Genes expression depleted in MK-STYX transfected cell lysate include cyclin dependent kinase inhibitor 2D (p19).

DISCUSSION

Pseudophosphatases are referred to as “dominant-negative” or non-functional proteins, which creates the impression that they do not play a role in the cell. This research is significant because it suggests a role for a pseudophosphatase. This thesis research demonstrates MK-STYX overexpression has an effect on the cell, particularly in stress response. MK-STYX decreases stress granule assembly; stress granules are dynamic storage sites for mRNA, and a protective response of the cell to stress. This evidence suggests MK-STYX could play a role in both stress granule assembly and disassembly.

MK-STYX and G3BP-1

Results from this research support the hypothesis that MK-STYX reduces stress granule assembly regardless of G3BP-1 phosphorylation status at site 149. Stress granule assembly is induced by G3BP-1 overexpression, and was thought to be dependent on dephosphorylation at serine 149. However, overexpression of MK-STYX inhibited the phosphomimetic G3BP-1 mutant (S149E) heat shock stress granules. This suggests that MK-STYX reduces stress granules regardless of G3BP-1 phosphorylation status.

Stress Granule Assembly

Further, this thesis observed that MK-STYX overexpression decreases phosphorylation of eIF2 α . This observation is subtle, but replicable. MK-STYX and eIF2 α were determined to interact from a co-immunoprecipitation study. This suggests that MK-STYX may decrease stress granule formation upstream of G3BP-1 aggregation. Through decreased phosphorylation and interaction with eIF2 α , MK-STYX may be regulating stress granule assembly.

It is intriguing that a pseudophosphatase, which is catalytically inactive, is causing decreased phosphorylation of eIF2 α . MK-STYX and eIF2 α interact, which could prevent phosphorylation necessary for stress granule formation. It is unlikely that the interaction between MK-STYX and eIF2 α leads to sequestering of eIF2 α , because that could deplete the cell of the translation initiation complex and induce stress granules. It is possible that MK-STYX could play the role of enhancing the activity of a phosphatase, or inhibiting a kinase (Figure 15). CReP or GADD34 bind with the PP1 catalytic subunit to directly regulate phosphorylation of eIF2 α . It is possible that a protein such as MK-STYX could play a role in regulating this pathway. For example, PTEN, a dual specificity phosphatase, is demonstrated as a regulator of CReP and eIF2 α phosphorylation (Zeng et al., 2011). Further, pseudophosphatases in *C. elegans* that are necessary for development have demonstrated the ability to bind a kinase and prevent substrate phosphorylation (Tonks, 2009). Another possibility for the

reduction of eIF2 α phosphorylation in the presence of MK-STYX is a feedback event. MK-STYX could reduce stress granules by another mechanism, such as promoting stress granule disassembly. This could lead to feedback that decreases eIF2 α phosphorylation, and at the same time MK-STYX could associate with eIF2 α in the process of stress granule disassembly.

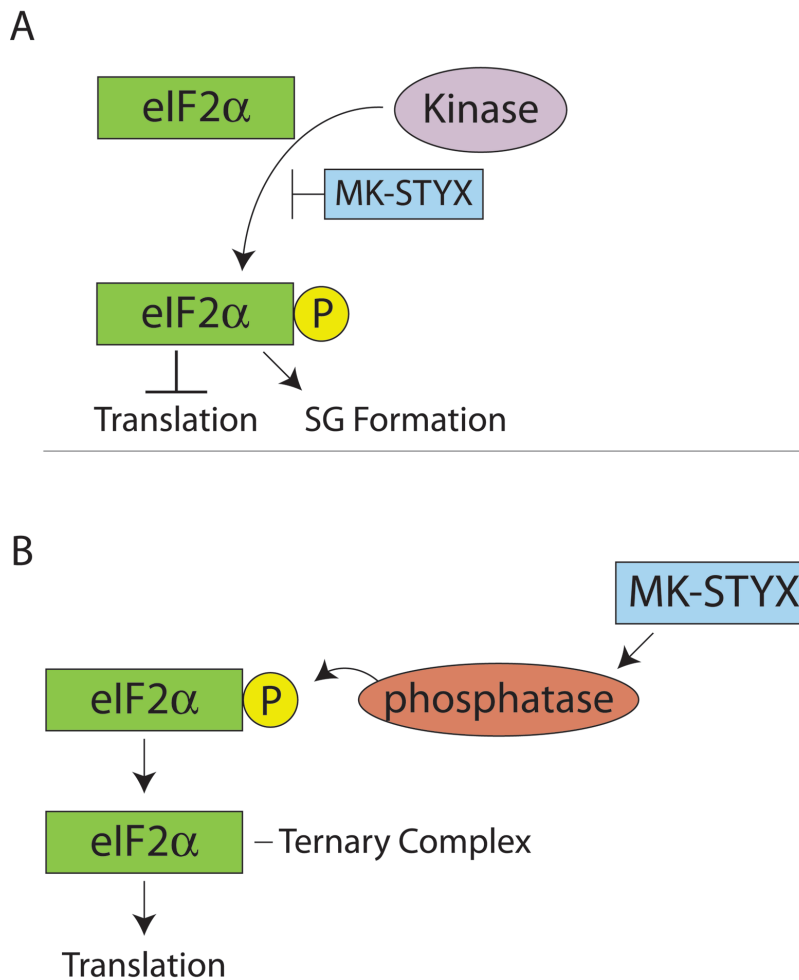


Figure 15. Alternative mechanisms of MK-STYX reduction of eIF2 α phosphorylation. (A) MK-STYX inhibits a kinase from phosphorylating eIF2 α , or (B) MK-STYX enhances the activity of a phosphatase to dephosphorylate eIF2 α

Stress Granule Disassembly

Research on stress granule disassembly is a current gap in the field, and the nature and kinetics of stress granule disassembly remains to be clarified. Heat shock stalls general translation, but selective translation for chaperones and proteins involved in the stress response persists. Hsp70 is needed for stress granule disaggregation. The data imply that MK-STYX could play a role in stress granule disassembly because Hsp70 expression is increased in the presence of MK-STYX. A future objective is to determine if MK-STYX interacts with Hsp70 by co-immunoprecipitation. This would confirm unpublished mass spectrometry results that MK-STYX and Hsp70 interact.

Characterizing MK-STYX

Subcloning, microarray and sequence and bioinformatics were used to gain insights about the function of MK-STYX. Subcloning to create a fusion protein that fluoresces red will determine the localization of MK-STYX in future studies. MK-STYX has been shown to localize to mitochondria (Niemi et al., 2011). It is important to determine if MK-STYX localizes to any other organelles, because cellular compartments have distinct functions in the cell, and can better indicate the function of MK-STYX. MK-STYX-Cherry will also be useful in determining if MK-STYX localizes to stress granules, and could allow for visualization of the role of MK-STYX in stress granule reduction.

Studying the amino acid sequence of MK-STYX indicates it is similar to MKPs but also points to important differences. Most importantly, MK-STYX lacks

the histidine and cysteine residues needed for nucleophilic attack in the PTP domain. However, this fold and the surrounding residues were still found as structurally related to dual specificity phosphatases and were recognized as a binding site for protein interactions by I-TASSER. These residues had a high Z-score, meaning that the model is a good prediction for the aligned residues. The residues that were problematic in sequence and structural comparisons are the residues where MK-STYX has CH2 domains. The CH2 domains of MK-STYX may not have the same function as other MKPs because MK-STYX does not have the KIM (kinase interaction motif) that MKP-1 and other MKPs use to bind MAPKs. Mutagenesis studies have shown that the KIM is necessary for highly specific binding that can differentiate between protein isoforms. The low confidence of predicted MK-STYX structures by I-TASSER is due to the inability to find a threading template for the CH2 regions. I-TASSER is also limited by the protein structures that have been experimentally crystalized. The structure of MKP-1 is not in the PDB library, and when its crystal structure is added greater insight into the structure of MK-STYX will be possible.

One surprising result from I-TASSER was Human TMDP (testis and skeletal muscle specific dual specificity phosphatase) as the second best structural analog of MK-STYX (Table 2). TMDP mRNA is found in spermatocytes at the beginning of meiosis, implicating its function is involved with spermatogenesis (Kim et al., 2007). The crystal structure of TMDP shows distinct structural motifs from other dual specificity phosphatases, resulting in a flat and

wide binding pocket so it shows no preference between pTyr or pThr residues (Kim et al., 2007). MK-STYX mRNA was found to be expressed in tissue of the testis by Northern Blot, and not in other tissues tested including brain, heart, kidney, liver, lung, skeletal muscle or spleen (unpublished data). Microarray showed PCTAIRE Kinase 1 is highly expressed in cells transfected with MK-STYX. PCTAIRE Kinase 1 is a poorly characterized protein that is essential for spermatogenesis (Mikolcevic et al., 2012). This result needs to be confirmed with further microarray experiments that optimize the protocol.

Future Directions and Implications

Other future objectives to better understand the role of MK-STYX and the mechanism of stress granule reduction include a more thorough study of eIF2 α phosphorylation. It is well cited in the literature, and demonstrated by the evidence provided in this thesis, that eIF2 α phosphorylation increases during heat shock. No study has determined which kinase is responsible for eIF2 α phosphorylation under these circumstances; however, it is usually implied to be PERK. Other details of eIF2 α phosphorylation and heat shock also should be determined. The degree of phosphorylation varies with the intensity of the stressor, so the temperature for heat shock and a time course of eIF2 α phosphorylation should be explored for this model. The cell's response to heat shock is dynamic and different depending on the organism, and maybe even cell type. Another important direction this project could take is to determine if MK-

STYX interacts with any other regulators of eIF2 α , such as PTEN (a dual specificity phosphatase), CReP or GADD34. Further studies include determining if MK-STYX is interacting with other proteins that G3BP-1 is known to complex with, such as OGFOD1. This complex has been implicating in regulating eIF2 α phosphorylation (Wehner, 2010).

In this thesis, G3BP-1 aggregation and stress granule formation has been shown with overexpression and heat shock. This verifies that in response to heat shock, cells assemble stress granules, and this observation demonstrates overexpressed G3BP-1 is recruited to stress granules during heat shock regardless of phosphorylation status. A future study to determine the role of endogenous G3BP-1 aggregation to stress granules during heat shock could be employed using a cell line stable transformed with GFP-tagged G3BP-1. Because there are other RNA-binding proteins recruited to stress granules, it would be interesting to see if endogenous G3BP-1 is always recruited to stress granules in response to heat shock, or if this only occurs from overexpression of G3BP-1. The current published literature suggests that G3BP-1 is always recruited to stress granules, but this is an important detail to verify in order to use G3BP-1 as a reliable marker of stress granules. Other RNA-binding proteins, such as TIA-1, are recruited to stress granules and are also commonly used as markers of stress granules.

Another study to determine if MK-STYX stabilizes polysomes will elucidate the role of MK-STYX. This study can be achieved by using fast protein liquid

chromatography (FPLC). If polysomes accumulate in the presence of MK-STYX, this could be interpreted as MK-STYX interfering in stress granule assembly. If polysomes do not accumulate, then MK-STYX may be more important in stress granule disassembly.

A systems biology study of MK-STYX implicated MK-STYX as a regulator of cell fate and apoptosis (Niemi et al., 2011). Stress granule formation and phosphorylation of eIF2 α are molecular mechanisms of cytoprotection. These mechanisms are abused in cells avoiding apoptosis. For example, cancer cells have high metabolic rates but are able to survive under stress by evading pro-apoptotic pathways. Chronic phosphorylation of eIF2 α may be an adaptive response of fast growing cells to stress (Zeng et al., 2011). Recruitment of specific proteins to stress granules suggests inhibition of apoptosis (Arimoto et al., 2008). The findings of this thesis, that MK-STYX plays a role in the stress response and regulates stress granules, are consistent with the idea that MK-STYX plays a role in cell fate and stress response.

Conclusion

It is important to continue studying MK-STYX, not only to clarify the mechanism of this protein in the stress response, but also to produce new knowledge for the scientific community studying cell signaling. There is a bias in molecular research to study proteins with known functions and avoid proteins with functions needing to be clarified. For the scientific community to better

understand fundamental biological mechanisms, it is important to study proteins with lesser-known functions to truly understand a pathway and a causal mechanism. The importance of understanding phosphatases and pseudophosphatases cannot be understated. Aberrant cell signaling leads to disease such as neurological degeneration and cancer; many cancer drugs are kinase inhibitors. Phosphatases are an endogenous check to kinase activity. Pseudophosphatases are catalytically inactive proteins with active phosphatase homologs. Pseudophosphatases cannot be overlooked when studying signaling molecules; the structural similarity to active homologs makes it likely that they are involved in cellular processes, and many, including MK-STYX, have multiple domains. High-throughput technology including genome sequencing, microarray, and mass spectrometry make it possible to produce a great amount of information about what is present and being expressed as protein in the cell. Understanding how these proteins act and fit together as pieces of a pathway is a challenge for researchers. Disease without an effective treatment or cure are a testament to the fact that there is a great deal in molecular biology that is not understood, and work on the lesser known proteins is exciting and worthwhile in efforts to understand signaling and disease.

References

- Andersen J.N., Jansen P.G., Echwald S., Mortensen O.H., Fukada T., Del Vecchio R., Tonks, N.K., and N.P.H. Møller. 2004. A genomic perspective on protein tyrosine phosphatases: gene structure, pseudogenes, and genetic disease linkage. *FASEB J.* 18(1): 8-30.
- Anderson P., and Kedersha N. 2002. Visibly stressed: the role of eIF2, TIA-1, and stress granules in protein translation. *Cell Stress Chaperones* 7(2):213-21.
- Anderson P., and N. Kedersha. 2009. Stress granules. *Curr Biol.* 19(10): R397-8.
- Bando Y., Onuki R., Katayama T., Manabe T., Kudo T., Taira K., and M. Tohyama. 2005. Double-stranded RNA dependent protein kinase (PKR) is involved in the extrastriatal degeneration in Parkinson's disease and Huntington's disease. *Neurochem Int.* 46(1): 11-8.
- Begley M.J., and J.E. Dixon. 2005. The structure and regulation of myotubularin phosphatases. *Curr Opin Struct Biol* 15(6):614-20.
- Blanchetot C., Chagon M., Dubé N., Hallé M., and M.L. Tremblay. 2005. Substrate-trapping techniques in the identification of cellular PTP targets. *Methods* 35(1): 44-53.
- Boudeau J., Miranda-Saavedra D., Barton G.J., and D.R. Alessi. 2006. Emerging roles of pseudokinases. *Cell Biol* 16(9): 443-452.
- Bugiani M., Boor I., Powers J.M., Scheper G.C., and M.S. van der Knaap. 2010. Leukoencephalopathy with vanishing white matter: a review. *J Neuropathol Exp Neurol.* 69(10): 987-96.
- Camps M., Nichols A., Gillieron C., Antonsson B., Muda M., Chabert C., Boschert U., and Arkinstall S. 1998. Catalytic activation of the phosphatase MKP-3 by ERK2 mitogen-activated protein kinase. *Science* 280(5367): 1262-5.
- Camps M., Nichols A., and Arkinstall S. 2000. Dual specificity phosphatases: a gene family for control of MAP kinase function. *FASEB J.* 14(1): 6-16.
- Chang R.C., Wong A.K., Ng H.K., and J. Hugon. 2002. Phosphorylation of eukaryotic initiation factor-2 α (eIF2 α) is associated with neuronal degeneration in Alzheimer's disease. *Neuroreport* 13(18):2429-32.

- Cheng K.C., Klancer R., Singson A., and G. Seydoux. 2009. Regulation of MBK-2/DYRK by CDK-1 and the pseudophosphatases EGG-4 and EGG-5 during oocyte-to-embryo transition. *Cell* 139(3): 560-72.
- Costa M., Ochem A., Staub A., and A. Falaschi. 1999. Human DNA helicase VIII: a DNA and RNA helicase corresponding to the G3BP protein, an element of the ras transduction pathway. *Nucleic Acids Res.* 27(3): 817-21.
- Denu J.M., Stuckey J.A., Saper M.A., and J.E. Dixon. 1996. Form and Function in Protein Dephosphorylation. *Cell* 87(3): 361-4.
- Dorfman K., Carrasco D., Gruda M., Ryan C., Lira S.A., and Bravo R. 1996. Disruption of the erp/mkp-1 gene does not affect mouse development: normal MAP kinase activity in ERP/MKP-1-deficient fibroblasts. *Oncogene* 13(5): 925-31.
- Farny N.G., Kedersha N., and P.A. Silver. 2009. Metazoan stress granule assembly is mediated by P-eif2 α -dependent and -independent mechanisms. *RNA* 15:1814-1821.
- Flint A.J., Tianis T., Barford D., and Tonks N.K. 1997. Development of "substrate-trapping" mutants to identify physiological substrates of protein tyrosine phosphatases. *Proc Natl Acad Sci.* 94(5): 1680-5.
- Gilks N., Kedersha N., Ayodele M., Shen L., Stoecklin G., Dember L.M., and Anderson P. 2004. "Stress granule assembly is mediated by prion-like aggregation of TIA-1. *Mol Biol Cell* 15(12): 5383-98.
- Harding H.P., Zhang Y., Scheuner D., Chen J.J., Kaufman R.J., and D. Ron. 2009. PP1r15 gene knockout reveals an essential role for translation initiation factor 2 alpha (eIF2alpha) dephosphorylation in mammalian development. *Proc Natl Acad Sci.* 106(6): 1832-7.
- Heinrich, R., B.G. Neel, and T.A. Rapoport. 2002. Mathematical models of protein kinase signal transduction. *Mol Cell.* 9:957-970.
- Hinton S.D., Myers M.P., Roggero V.R., Allison L.A., and N.K. Tonks. 2010. The pseudophosphatase MK-STYX interacts with G3BP and decreases stress granule formation. *Biochem J* 427(3): 349-57.
- Irvine K., Stirling R., Hume D., and D. Kennedy. 2004. Rasputin, more promiscuous than ever: a review of G3BP. *Int J Dev Biol* 48(10): 1065-77.

- Kedersha, N.L., M. Gupta, W. Li, I. Miller, and P. Anderson. 1999. RNA-binding proteins TIA-1 and TIAR link the phosphorylation of eIF-2 alpha to the assembly of mammalian stress granules. *J Cell Biol.* 147:1431-1442.
- Kedersha, N. Cho M.R., Li W., Yacono P.W., Chen S., Gilks N. Golan D.E., and P. Anderson. 2000. Dynamic shuttling of TIA-1 accompanies the recruitment of mRNA to mammalian stress granules. *J Cell Biol.* 151(6): 1257-68.
- Kedersha N., Chen S., Gilks N., Li W., Miller I.J., Stahl J., and P. Anderson. 2002. Evidence that ternary complex (eIF2-GTP-tRNA(i)(Met))-deficient preinitiation complexes are core constituents of mammalian stress granules. *Mol Biol Cell* 13(1): 195-210.
- Kedersha N., Stoecklin G., Ayodele M., Yacono P., Lykke-Andersen J., Pritzler M.J., Scheuner D., Kaufman R.J., Golan D.E., and P. Anderson. 2005. Stress granules and processing bodies are dynamically linked sites of mRNP remodeling. *J Cell Biol* 169(6):871-84.
- Kim S.J., Jeong D.G., Yoon T.S., Son J.H., Cho S.K., Ryu S.E., and J.H. Kim. 2007. Crystal structure of human TMDP, a testis-specific dual specificity protein phosphatase: implications for substrate specificity. *Proteins* 66(1): 239-45.
- Leblanc, V., Tocque B., and I. Delumeau. 1998. Ras-GAP controls Rho-mediated cytoskeletal reorganization through its SH3 domain. *Mol Cell Biol.* 18(9): 5567-5578.
- Leblanc V., Delumeau I., and B. Tocqué. 1999. Ras-GTPase activating protein inhibition specifically induces apoptosis of tumour cells. *Oncogene.* 18(34): 4884-9.
- Mazroui R., Huot M.E., Tremblay S., Filion C., Labelle Y., and E.W. Khandjian. 2002. Trapping of messenger RNA by Fragile X Mental Retardation protein into cytoplasmic granules induces translation repression. *Hum Mol Genet* 11(24): 3007-17.
- Mikolcevic P., Sigl R., Rach V., Hess M.W., Pfaller K., Barisic M., Pelliniemi L.J., Boesl M., and S. Geley. 2012. Cyclin-dependent kinase 16/PCTAIRE kinase 1 is activated by cyclin Y and is essential for spermatogenesis. *Mol Cell Biol* 32(4):868-79.
- Muda M., Theodosiou A., Gillieron C., Smith A., Chabert C., Camps M., Boschert U., Rodrigues N., Davies K., Ashworth A., and S. Arkinstall. 1998. The mitogen-activated protein kinase phosphatase-3 N-terminal noncatalytic region is responsible for tight substrate binding and enzymatic specificity. *J Biol Chem.* 273(15): 9323-9.

- Neel, B.G., and N.K. Tonks. 1997. Protein tyrosine phosphatases in signal transduction. *Curr Opin Cell Biol.* 9(2): 193-204.
- Niemi N.M., Lanning N.J., Klomp J.A., Tait S.W., Xu Y., Dykema K.J., Murphy L.O., Gaither L.A., Xu H.E., Furge K.A., Green D.R., and J.P. MacKeigan. 2011. MK-STYX, a catalytically inactive phosphatase regulating mitochondrially dependent apoptosis. *Mol Cell Biol.* 31(7): 1357-68.
- Owens D.M., and Keyse S.M. 2007. Differential regulation of MAP kinase signaling by dual-specificity protein phosphatases. *Oncogene.* 26: 3203-3213.
- Parker, F., F. Maurier, I. Delumeau, M. Duchesne, D. Faucher, L. Debussche, A. Dugue, F. Schweighoffer, and B. Tocque. 1996. A Ras-GTPase-activating protein SH3-domain-binding protein. *Mol Cell Biol.* 16:2561-2569.
- Parry J.M., Velarde N.V., Lefkovith A.J. Zegarek M.H., Hang J.S., Ohm J., Klancer R., Maruyama R., Druzhinina M.K., Grant B.D., Piano F., and A. Singson. EGG-4 and EGG-5 Link Events of the Oocyte-to-Embryo Transition with Meiotic Progression in *C. elegans*. *Curr Biol* 19(20): 1752-7.
- Peel A.L. 2004. PKR activation in neurodegenerative disease. *J Neuropathol Exp Neurol* 63(2):97-105.
- Petsko G.A., and D. Ringe. 2004. Protein structure and function. New Science Press, Ltd: Sunderland, Mass.
- Richter K., Haslbeck M., and J. Buchner. 2010. The heat shock response: life on the verge of death. *Mol Cell* 40: 253-366.
- Robinson F.L., and J.E. Dixon. 2005. The phosphoinositide-3-phosphatase MTMR2 associates with MTMR13, a membrane-associated pseudophosphatase also mutated in type 4B Charcot-Marie-Tooth disease. *J Biol Chem* 280(36): 31699-707.
- Roy A., Kuckukural A., and Y. Zhang. 2010. I-TASSER: a unified platform for automated protein structure and function prediction. *Nature Protocols* 5(4): 725-738.
- Silligan, C., Ban J., Bachmaier R., Spahn L., Kreppel M., Schaefer K.L., Poremba C., Aryee D.N., and H. Kovar. 2005. EWS-FLI1 target genes recovered from Ewing's sarcoma chromatin. *Oncogene* 24(15): 2512-24.

- Sun, H., Charles C.H., Lau, L.F., and N.K. Tonks. 1993. MKP-1 (3CH134), an immediate early gene product, is a dual specificity phosphatase that dephosphorylates MAP kinase in vivo. *Cell* 75(3): 487-93.
- Thomas M.G., Martinez T.L.J., Loschi M., Pasquini J.M., Correale J., Kindler S., and G.L. Boccaccio. 2005. Staufen recruitment into stress granules does not affect early mRNA transport in oligodendrocytes. *Mol Biol Cell* 16(1): 405-20.
- Tocque B., Delumeau I., Parker F., Maurier F., Multon M.C., and F. Schweighoffer. 1997. Ras-GTPase activating protein (GAP): a putative effector for Ras. *Cell Signal* 9(2):153-8.
- Tonks, N.K. 2006. Protein tyrosine phosphatases: from genes, to function, to disease. *Mol Cell Biol.* 7(11):833-46.
- Tonks, N.K. 2009. Pseudophosphatases: Grab and hold on. *Cell* 139(3): 464-5.
- Tourriere, H., K. Chebli, L. Zekri, B. Courselaud, J.M. Blanchard, E. Bertrand, and J. Tazi. 2003. The RasGAP-associated endoribonuclease G3BP assembles stress granules. *J Cell Biol.* 160:823-831.
- Wehner K.A., Schütz S., and P. Sarnow. 2010. OGFOD1: A novel modulator of eIF2 α phosphorylation and the cellular response to stress. *Mol Cell Biol.* 30(8):2006-16.
- Wiseman R.L., and J.W. Kelly. 2011. Phosphatase inhibition delays translational recovery. *Science* 332(6025):44-5.
- Wishart M.J., and Dixon J.E. 1998. Gathering STYX: phosphatase-like form predicts functions for unique interaction domains. *Trends Biochem Sci* 23(8): 301-6.
- Wishart M.J., and Dixon J.E. 2002. The archetype STYX/dead-phosphatase complexes with a spermatid mRNA-binding protein and is essential for normal sperm production. *Proc Natl Acad Sci* 99(4): 2112-7.
- Zeng N., Li Y., He L., Xu X., Galicia V., Deng C., and B.L. Stiles. 2011. Adaptive basal phosphorylation of eIF2 α is responsible for resistance to cellular stress-induced cell death in Pten-null hepatocytes. *Mol Cancer Res.* 9(12): 1708-17.